

**ABSORBANCE-BASED ASSAY FOR THE DETECTION OF MEMBRANE
DISRUPTION OF PYRROLOQUINOLINE QUINONE ENCAPSULATED
LIPOSOMES**

Brittany Virginia Worley

Senior Honors Thesis

19 April 2011

University of Michigan Department of Chemistry

This thesis has been read and approved by _____ . Date: __/__/__

ACKNOWLEDGEMENTS

My four years at the University of Michigan have been a complete whirlwind of small victories, sleepless nights, excitement, stress, laughter, and tears, and through all of this I have been surrounded by an immense support system that has helped me along as I've grown both personally and academically. First, I would like to thank Dr. Mark Meyerhoff, whose guidance and advice over the past three years has directed me towards becoming the type of scientist I want to be. Working in the Meyerhoff lab has been an incredibly rewarding experience, and one of the best decisions I've made here at Michigan. Next, I would like to thank my graduate student mentor, Laura Zimmerman, for taking me in and teaching me the wonders of working with liposomes. Laura has not only been a wonderful asset in helping me navigate through my undergraduate chemistry career, but she has become a beloved friend and role model. Thanks, L, you're the best. Similarly, I would like to thank Natalie Walker, who became a second mentor to me as well as a wonderful friend; I am incredibly grateful for all you have done for me.

I would also like to thank all the members of the Meyerhoff group, both past and present, who were always willing to answer a question or share a laugh. Working in this lab has been such a fantastic experience for me, and it is really the group members who have made it such a memorable time. Also, much of my work with liposomes was done in Dr. Lee's lab in the School of Pharmacy, and I am incredibly grateful to the entire Lee group, especially Chet Provoda, for allowing me to invade their lab from time to time and pester them all with questions. Finally, I owe thanks to Bev Lange in the chemistry office, who may be the best boss anyone could have and has absolutely the greatest, most infectious laugh ever.

I also owe thanks to all of my friends, who may not have understood why I spent so many hours in lab or got overly excited about a periodic table shower curtain, but were always there by

my side to pick me up when I got too bogged down. I would like to give special thanks to Elise Brown, Jeannie Lieder, Alex Levy, Kelsey Clancy, and Dan Cook. Elise, thank you for always knowing when I need my spirits lifted and how to do it, and for managing to live in the same room as me for two years and still be my friend at the end. Jeannie, I am ever grateful for your endless supply of support and encouragement in every aspect of my life, as well as your tough love when I need it. Alex, thank you for listening to every single complaint I've had in the past three years, and then for helping me to forget them. Kelsey, thank you for being my angel, for understanding me when I can't understand myself, and for showing me there is real love in this world. And finally Dan, thank you for knowing how to make me smile and for being that little bit of reason and sensibility amidst all the crazy in my world. You have all been an important part of my life, and I hope you know how much I have appreciated the support, friendship, and love you have given me over the past few years.

Lastly, I would like to send thanks and love to my family. To my parents, Keith and Sara, who have supported me in all of my endeavors, given me good advice (whether or not it was asked for), and taught me to stand strong against all odds and fight for what I believe. Your love and guidance has helped me through both good and bad, and I owe you everything. I would also like to thank my brother Eric, who has become one of my best friends despite his ability to drive me absolutely insane, and my cousin Meghan, for her constant love and support and for being my big sister and best friend. Finally, thank you to my grandmother, aunts, uncles, and cousins for always supporting and believing in me. It is with the help this fantastic system of support that I have come this far, and I appreciate every one of you.

TABLE OF CONTENTS

ACKNOWLEDGEMENTS.....	1
LIST OF FIGURES.....	4
LIST OF TABLES.....	7
ABSTRACT.....	8
INTRODUCTION.....	10
MATERIALS AND METHODS.....	22
RESULTS AND DISCUSSION.....	32
<i>Evaluation of Antimicrobial Peptide Activity</i>	36
<i>Evaluation of Synthetic Copolymer Activity</i>	40
<i>Evaluation of DNP Model System for Complement Fixation Testing</i>	47
CONCLUSION.....	55
REFERENCES.....	57

LIST OF FIGURES

- Figure 1:** Membrane permeabilization by antimicrobial peptides
- Figure 2:** Base structure of methacrylamide copolymers⁷
- Figure 3:** Mechanism of platelet lysis in HIT¹⁴
- Figure 4:** Complement fixation test – serum with and without antibodies
- Figure 5:** Structure of a liposome
- Figure 6:** Structure of PQQ
- Figure 7:** Ribbon structure of activated GDH dimer²⁴
- Figure 8:** PQQ reconstitution optical assay concept
- Figure 9:** Dose-response of optical assay ranging from 0 nM to 2.5 nM PQQ
- Figure 10:** HIT diagnostic assay concept
- Figure 11:** PQQ assay membrane permeabilization concept
- Figure 12:** Liposome composition optimization
- Figure 13:** Structures of egg PC, DOPA, and cholesterol
- Figure 14:** Stability of egg PC, DOPA, and cholesterol liposomes after 3 weeks
- Figure 15:** Average liposome size
- Figure 16:** Free PQQ calibration curve
- Figure 17:** Liposome concentration optimization
- Figure 18:** Dose response of MSI-594 and MSI-78, as compared to rIAPP (egg PC/POPG liposomes)

- Figure 19:** Selectivity of MSI-594 and MSI-78 response over rIAPP (egg PC/POPG liposomes)
- Figure 20:** Initial and final images of kinetic dose-response assay (egg PC/POPG liposomes)
- Figure 21:** Dose-response of MSI-594 compared to rIAPP (egg PC/DOPA/chol. liposomes)
- Figure 22:** Dose-response of MSI-78 compared to rIAPP (egg PC/DOPA/chol. liposomes)
- Figure 23:** MSI-594 endpoint assay (egg PC/POPG liposomes)
- Figure 24:** Initial and final images of MSI-594 endpoint assay (egg PC/POPG liposomes)
- Figure 25:** Structure of fluorescent dye HPTS
- Figure 26:** Fluorescent detection of MSI-594 using HPTS-encapsulated liposomes
- Figure 27:** Structures of POPE and POPG lipids
- Figure 28:** PH series kinetic assay (POPE/POPG liposomes)
- Figure 29:** PB series kinetic assay (POPE/POPG liposomes)
- Figure 30:** Comparison of PH and PB series with varying f_{alkyl} values (POPE/POPG liposomes)
- Figure 31:** PH series kinetic assay (egg PC/DOPA/chol liposomes)
- Figure 32:** PB series kinetic assay (egg PC/DOPA/ chol liposomes)
- Figure 33:** Comparison of PH and PB series with varying f_{alkyl} values (egg PC/DOPA/chol liposomes)
- Figure 34:** Initial and final images of PH and PB series kinetic assay (POPE/POPG liposomes)
- Figure 35:** Linear dose-response of PH₅₁ and PB₅₄ (egg PC/DOPA/chol liposomes)
- Figure 36:** PH₅₁ and PB₂₀ endpoint assay (POPE/POPG liposomes)

- Figure 37:** Initial and final images of PH₅₁ and PB₂₀ endpoint detection (POPE/POPG liposomes)
- Figure 38:** PH₅₁ and PB₅₄ endpoint assay (egg PC/DOPA/chol liposomes)
- Figure 39:** Structures of DOPG, Lysyl-DOPG, and cardiolipin
- Figure 40:** Membrane permeabilization of gram-positive cell mimics
- Figure 41:** Structure of DNP-containing liposomes
- Figure 42:** Aggregation of egg PC, cholesterol, and DNP PE liposomes in solution
- Figure 43:** Stability of 33:33:33:1 mole % egg PC:DOPA:cholesterol:DNP PE liposomes after 3 weeks
- Figure 44:** Stability of 44:44:11:1 mole % egg PC:cholesterol:DOPA:DNP PE liposomes after 3 weeks
- Figure 45:** Comparison of DNP PE and DNP Cap PE lipid structures
- Figure 46:** UV-visible spectrum of egg PC, DOPA, and cholesterol liposomes
- Figure 47:** UV-visible spectrum of egg PC, DOPA, cholesterol, and DNP PE liposomes
- Figure 48:** Competitive binding assay concept
- Figure 49:** Competitive binding assay: egg PC, DOPA, and cholesterol liposomes with and without DNP
- Figure 50:** Representative spectrum of DNP system kinetic response

LIST OF TABLES

- Table 1:** Peptide Sequences²⁶
- Table 2:** Copolymer structure and degree of alkylation⁷
- Table 3:** Liposome Characteristics
- Table 4:** DNP Liposome Compositions

ABSTRACT

This thesis describes an optical homogeneous assay that uses the enzyme reconstitution reaction of the prosthetic group pyrroloquinoline quinone (PQQ) with apo-glucose dehydrogenase (apo-GDH) for the detection of bilayer membrane permeabilization by antimicrobial peptides, synthetic copolymers, and complement fixation. Liposomes, small spheres made of lipid bilayers, are employed to encapsulate PQQ as a tracer. When PQQ is released through the bilayers of the liposomes by a given species, it binds to apo-GDH and activates the catalytic center. PQQ acts as a redox center in this enzyme, catalyzing the oxidation of glucose to glucono lactone. A redox dye, dichlorophenol indophenol (DCPIP) is introduced to the assay mixture, which changes color from blue in its oxidized form to colorless when reduced by PQQ. The color change due to the reduction of DCPIP is measured via an optical absorbance assay.

PQQ-loaded liposomes and a membrane permeabilizing agent are added to the wells of a microtiter plate. The concentration of peptide or polymer alters the rate of membrane permeabilization, releasing PQQ, which is detected by the DCPIP color change. For quantitative measurements, the absorbance change over a 30 min time period was measured. This absorbance change is related to the relative membrane permeabilizing activity and concentration of the antimicrobial agent. By varying the liposome composition, both the antimicrobial activity and the potential toxicity towards mammalian cells of these agents can be evaluated.

This thesis also discusses the potential adaption of the absorbance-based PQQ assay to combine with complement fixation to develop a diagnostic assay for heparin-induced thrombocytopenia (HIT). A model system using liposomes with a 2,4-dinitrophenyl (DNP) containing lipid is used as an initial model. The DNP molecules are present on the surface of the

liposomes, and therefore should complex to anti-DNP antibodies in solution. The addition of complement in the presence of anti-DNP should result in liposome lysis, while addition without anti-DNP should not cause liposome lysis.

INTRODUCTION

Antibacterial Resistance

Since A. Fleming's discovery of the antibacterial activity of penicillin in 1929¹, antibiotics have become standard in the treatment of bacterial infection. Recently, however, antibacterial resistance has grown, due to both the evolution of bacterial strains and the misuse of antibiotics, resulting in a class of bacterial infections that cannot be treated by traditional antibiotics. Because of this resistance, there is a growing need for the development of new antimicrobial therapeutic agents.

Antimicrobial Peptides

One type of new therapeutic agents being developed is antimicrobial peptides². Antimicrobial peptides are naturally present in the immune systems of various organisms³, functioning as a natural defense mechanism by killing foreign cells. When found in nature, the sequences of antimicrobial peptides are so diverse that the same sequence is rarely found in multiple species of animals; the diversity of these peptides is enhanced by synthetic manufacture in laboratories. Despite this diversity, however, antimicrobial peptides are almost all composed of hydrophilic, hydrophobic, and cationic amino acids organized in an amphipathic structure⁴.

These peptides function by targeting foreign microbes and binding to their exterior membranes, subsequently permeating the cell membrane and destroying the cell. The membrane of the foreign cell is lysed through

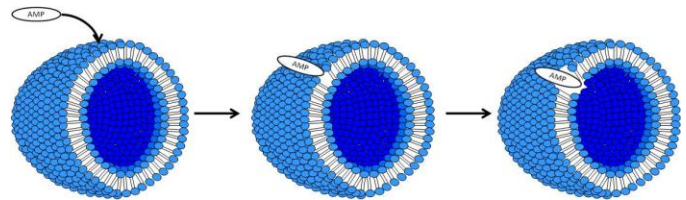


Figure 1: Membrane lysis by antimicrobial peptides. Peptides compromise the membrane of the foreign cell by replacing the lipids composing the outer layer.

interaction with the antimicrobial peptide, which leads to a displacement of the membrane lipids and alters the overall membrane structure⁴ (Figure 1).

The use of antimicrobial peptides as antibacterial therapeutic agents is potentially superior to that of traditional antibiotics due to their wide range of antibacterial activity and applicability. Furthermore, it has been shown that antimicrobial peptides not only kill bacteria faster than antibiotics, but they continue to be effective in fighting bacterial strains already resistant to traditional treatments⁵. As a result of their effectiveness against bacterial infections, synthetic antimicrobial peptides are currently being developed, resulting in the need to devise a fast and simple method for screening the antimicrobial activity of new peptides on both gram positive and gram negative bacteria, as well as the toxicity of new peptides against mammalian cells.

Synthetic Copolymers

In addition to the work being done with antimicrobial peptides, efforts have been made to create synthetic polymers that display similar antimicrobial properties. The low molecular weight copolymers developed by Kuroda et al. have been shown to demonstrate antimicrobial activity through a mechanism that involves the disruption of cell membranes⁶⁻⁷. These methacrylamide copolymers are comprised of hydrophobic backbones with side chains consisting of protonated primary amine groups and hydrophobic alkyl groups. The

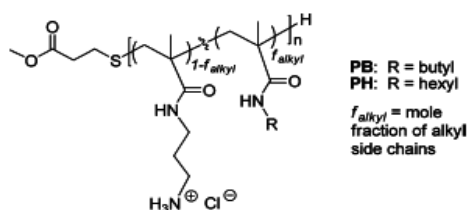


Figure 2: Base structure of methacrylamide random copolymers. R is either butyl (PB series) or hexyl (PH series). f_{alkyl} is the mole fraction of alkyl side chains.

hydrophobicity of the copolymers is determined by the mole fraction of the alkyl side chains (f_{alkyl}), as well as their length (Figure 2). Increasing the mole fraction and length of the alkyl side chains increases the copolymer's hydrophobicity, which increases the polymer's

antimicrobial activity against *Escherichia coli* and *Staphylococcus aureus*. However, it has been demonstrated that excessive hydrophobicity can result in increased hemolytic activity and the lysis of human cells. Therefore, structure optimization is required to balance the hydrophobicity and cationic charge in order to maximize the polymer's selectivity for bacterial cells over human cells. Due to this need for optimization, a simple, high-throughput method for determining the antimicrobial and hemolytic activity of copolymers of varied hydrophobicity is desirable.

Current Detection Methods

Current methods used to detect membrane permeabilization by antimicrobial peptides and polymers are typically based on the efflux of fluorescent dyes, most often calcein or carboxyfluorescein, encapsulated in liposomes⁸ (small shells consisting of phospholipid bilayers often used as analytical cell mimics). Prior to membrane permeabilization, the fluorescent signal is quenched. Furthermore, because the fluorescence of these dyes is concentration-dependent, as more dye is released due to membrane permeabilization, an increase in fluorescence is observed⁸⁻⁹. These fluorescent methods, however, are disadvantageous because they require expensive microtiter type instrumentation for fluorescent detection and readout.

A visual detection method for membrane permeabilization, based on the fluorescence emission of terbium(III) (Tb^{3+}) chelated with dipicolinic acid (DPA), has also been documented¹⁰. The binary Tb^{3+} /DPA complex emits bright green fluorescence when irradiated with UV light, removing the need for expensive instrumentation. In this method, unilamellar phospholipid vesicles encapsulate either a solution of Tb^{3+} or DPA, with the conjugate molecule in the external solution. After membrane permeabilization, the interior solution is released and the fluorescing complex formed, resulting in a visibly fluorescent solution. Using the

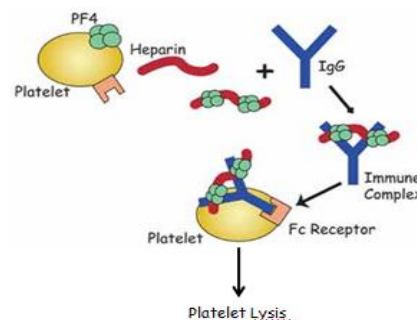
antimicrobial peptide alamethicin, this method was demonstrated to visually detect membrane permeabilization with high sensitivity and low limits of detection. However, because the Tb^{3+} /DPA complex excites in the UV region of the spectrum, quantitative studies for this method are difficult without expensive quartz microtiter plates and instrumentation.

The methodologies currently in use for detecting membrane permeabilization are lacking a sensitive visual detection method that can easily be adapted for both low cost qualitative studies and high throughput screening of new peptides and polymers exhibiting antimicrobial behavior.

Heparin Induced Thrombocytopenia (HIT)

Heparin induced thrombocytopenia (HIT) is a side effect of the administration of the anticoagulant heparin that results in the development of low platelet counts about 5-10 days after the start of heparin therapy¹¹. In HIT, heparin complexes to platelet factor 4 (PF4), which results in the formation of IgG antibodies directed toward that complex by the body's immune system.

These IgG antibodies bind to the heparin-PF4 complexes on the surface of platelets in the bloodstream. The antibody tail binds to the FcγIIa receptor on the surface of platelets, resulting in platelet activation and lysis¹² (Figure 3) When a



patient is suspected of displaying complications related to HIT, an accurate confirmation of the diagnosis is required to begin the proper treatment. However, no specific laboratory test is available and is broadly used for HIT diagnosis.

Figure 3: Mechanism for platelet lysis in HIT. Heparin and PF4 create a complex with IgG antibodies, which aggregate on the platelet surface and lead to lysis.

Current Detection Methods

The most common method used for HIT diagnosis is enzyme-linked immunosorbent assay (ELISA), which is used to detect anti-heparin/PF4 antibodies in serum¹³. Despite its sensitivity, this method lacks specificity¹¹ because the immunoassay detects all circulating antibodies that bind to heparin-PF4 complexes and falsely identifies antibodies that do not cause HIT.

The serotonin-release assay (SRA) is the most specific test for HIT diagnosis. This assay measures platelet release/activation, as opposed to aggregation, at two heparin concentrations¹⁵. However, despite the specificity of this assay, it is used by only a few laboratories worldwide because it requires radioactive material and proficient human skill to be reproducible¹³. Other functional methods can be used to confirm HIT, such as the particle agglutination assay and flow cytometry. Both of these, however, provide variable results, and in aggregometry in particular the results are not standard, but depend strongly on the patient. All three of these assays lack sensitivity and are often indeterminate in the first two days of HIT¹³.

The current methods used to diagnose HIT lack either sensitivity or specificity. As such, the development of a simple and sensitive diagnostic assay is needed that is potentially more specific for HIT antibodies.

Complement Fixation

A possible method for the detection of HIT antibodies would be an adaptation of complement fixation. The complement fixation test is used to detect the presence of specific antibodies or antigens in serum in order to diagnose infections¹⁶. The assay uses sheep red blood cells (sRBC) bound to anti-sRBC antibody and complement to determine whether or not a specific antibody is present in a patient's serum. If the antibody is present, addition of the

specific antigen will form antibody-antigen complexes that will bind to the complement in

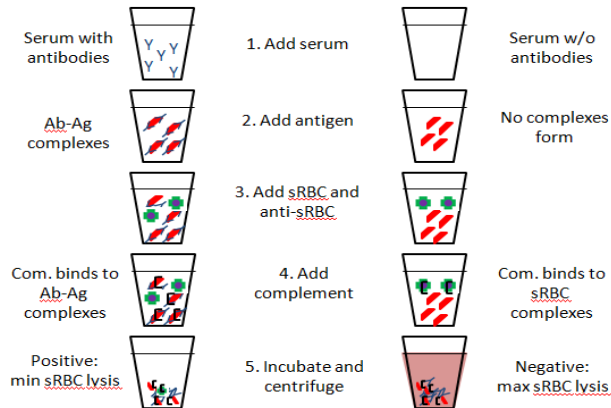


Figure 4: Complement fixation test. When antibodies are not present, the addition of complement leads to maximum sRBC lysis and a negative test. In the presence of antibodies, complement binds to the antigen-antibody complex, resulting in minimal sRBC lysis and a positive test.

solution, resulting in minimal lysis of the sRBC complexes. If the antibody is not present, the addition of antigen will not result in the formation of complexes, causing the complement to bind to sRBC complexes and leading to maximal sRBC lysis. In this way, a test that is negative for a given antibody results in lysis while a positive test does not (Figure 4).

Adaptation of the complement fixation test using liposomes in place of sRBCs may allow for a selective diagnostic assay for HIT.

Liposomes

In order to increase sensitivity and decrease detection limits of bioassays, the development of new labeling strategies that exhibit an increased signal over traditional labeling techniques has become an emergent trend. One strategy to increase signal is to develop labels that are capable of delivering multiple tracer molecules for each binding event, through either encapsulation of

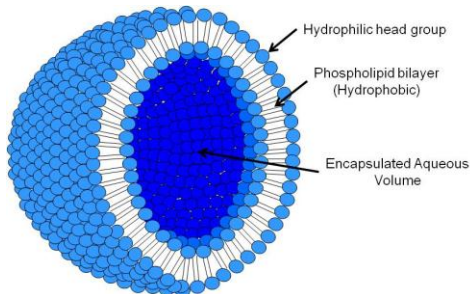


Figure 5: Liposome structure. The hydrophilic lipid head group is present on the outer and inner surface of the liposome, with a hydrophobic phospholipid bilayer in between. An aqueous volume is encapsulated in the liposome interior.

tracer molecules or their conjugation to the exterior or a labeling entity. Liposomes, first introduced in 1965¹⁷, are one such labeling method capable of delivering hundreds to thousands of tracer molecules per binding event.

Liposomes are small spheres made of phospholipid

bilayers encapsulating a small aqueous volume, which can effectively contain any small hydrophilic molecule (Figure 5). Their encapsulation abilities have made liposomes fairly prevalent in the pharmaceutical industry as a vehicle for drug delivery. The liposome's ability to deliver a large number of tracer molecules per each binding event has also led to the widespread use of these analytical reagents in both immunoassays and DNA assays¹⁸⁻²⁰. Furthermore, because liposomes can be formed using various lipid compositions, they can be used as any number of bacterial and mammalian cell mimics.

In these assays, the encapsulated tracers are most often fluorophores, chemiluminescent dyes, and reduction/oxidation reactive species. Upon permeabilization of the lipid bilayer, these species are released and can be detected using various detection methods. Beyond encapsulation of the tracer molecule, tracer entities such as enzymes can be conjugated to the surface of the liposome shell and detected without disrupting the lipid bilayer.

Enzymes and Prosthetic Groups

A new class of potential tracer molecules is enzyme prosthetic groups, which are small organic molecules that bind to the active site of an enzyme. The binding of the prosthetic group to an enzyme activates the enzyme by facilitating its specific functionality; without the prosthetic group present, the enzyme is inactive. The protein portion of the inactive enzyme, without the prosthetic group, is called the apo-enzyme. Once the prosthetic group is bound and the enzyme activated, it is referred to as the holo-enzyme. The process of a prosthetic group binding to the apo-enzyme and activating it is called reconstitution.

The binding of a prosthetic group to an enzyme can be either non-covalent (through hydrogen bonding or electrostatic interactions) or covalent (via amino acid residues), and is a

highly specific process resulting in tight bonding between the prosthetic group and the enzyme. Because of this, reconstitution can be used as a platform for detecting the concentration of a particular prosthetic group, and has been applied to binding and immunoassays.

One particular assay is based on the reconstitution of apo-glucose oxidase using the prosthetic group flavin adenine dinucleotide (FAD)²¹. In this homogeneous colorimetric immunoassay, a ligand-FAD complex (without antibody) is bound by apo-glucose oxidase; the activity of the reconstituted holo-glucose oxidase can be monitored through the hydrogen peroxide generated by the enzymatic reaction. A prototype immunoassay for the drug theophylline in human serum was developed. The binding of anti-theophylline antibodies to the theophylline-FAD conjugate prevented the reactivation of the apo-enzyme. When theophylline was present in the sample, however, competitive binding allowed some of the FAD complex to reactivate the apo-enzyme, resulting in enzyme activity proportional to the amount of free theophylline in the sample. Based on this, it can be seen that the amount of enzyme reconstitution is directly related to the concentration of free analyte in the sample.

Pyrroloquinoline Quinone (PQQ) and Glucose Dehydrogenase (GDH)

Pyrroloquinoline Quinone (PQQ) is a quinone prosthetic group that was discovered in 1979²², and is present in a variety of bacteria (Figure 6). PQQ non-covalently binds as a cofactor to a large subgroup of quinoproteins, which are enzymes that oxidize certain alcohols and amines once activated by a quinone prosthetic group. Glucose dehydrogenase (GDH) is one of the quinoproteins that tightly binds PQQ in its active site; once bound, GDH is activated and is capable of oxidizing a wide array of mono- and disaccharides into their

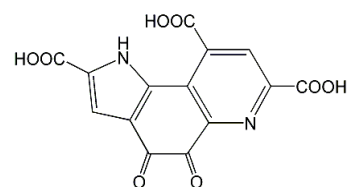
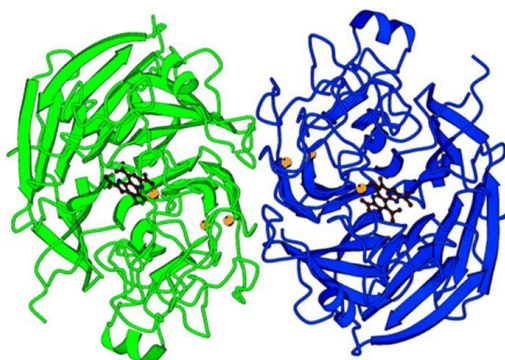


Figure 6: PQQ structure. At neutral pH=7, PQQ has a 3- charge.

corresponding ketones²³. Specifically, holo-GDH catalyzes the oxidation of glucose into glucono lactone²³.

Upon activation, GDH forms a dimer with one PQQ molecule and three calcium ions (Ca^{2+}) bound per each 50kDa enzyme monomer²⁴ (Figure 7). The calcium ions are required to both activate the PQQ prosthetic group and facilitate the dimerization of the GDH monomers. Once activated, the PQQ molecules act as reduction and oxidation centers, with the PQQ



Yellow spheres represent Ca^{2+}

Figure 7: Structure of GDH dimer. Ca^{2+} facilitates the dimerization of the enzyme. Two PQQ molecules are bound in each dimer, creating catalytic centers.

molecule itself capable of repeat redox cycling. In the presence of glucose, for example, PQQ undergoes a two electron reduction as a result of the oxidation of glucose to glucono lactone.

Colorimetric Detection of PQQ

The PQQ/apo-GDH reconstitution reaction has previously been adapted to a heterogeneous colorimetric binding assay, where PQQ-doped nanospheres are used as analytical reagents²⁵. In this assay, C-reactive protein (CRP) was detected using neutravidin-coated, PQQ-loaded poly(methyl methacrylate) nanospheres, which bind with a biotinylated CRP reporter antibody causing the encapsulated PQQ to be released. The released PQQ reconstitutes the apo-GDH; when excess glucose and the colored redox dye 1,6-dichlorophenol indophenol (DCPIP) are added to the assay, a color change indicating the presence of free PQQ occurs. In the absence of PQQ, the inactive GDH does not facilitate the enzymatic reaction and no color change is observed.

The observed color change is based on the reduction/oxidation cycle that takes place between PQQ, glucose, and DCPIP. Upon lysis, PQQ is released from the nanospheres, at which point the free PQQ binds to the GDH present in solution, facilitated by free calcium chloride in

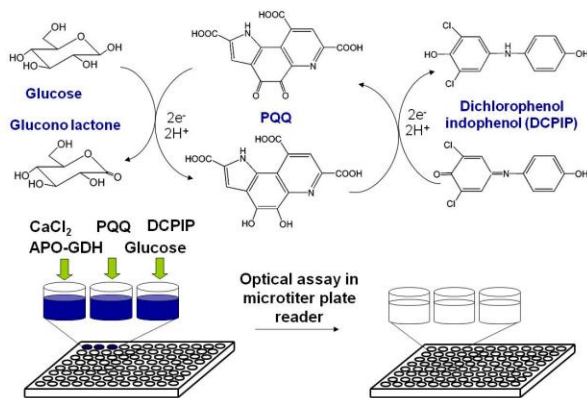


Figure 8: PQQ reconstitution assay concept. The two electron redox cycle between glucose, PQQ, and DCPIP results in a color change from dark blue to colorless.

assay measures the color change that occurs while DCPIP is reduced; a calibration curve of free PQQ is shown in Figure 9 to demonstrate the sensitivity and speed of this colorimetric assay. Furthermore, the color change caused by the reduction of DCPIP can be observed without instrumentation, allowing for inexpensive and easy detection of PQQ.

Statement of Research

The main focus of this research is to further adapt the simple colorimetric detection of PQQ to a homogeneous microtiter plate assay for the detection of membrane permeabilization by antimicrobial peptides and copolymers. PQQ-loaded liposomes are used to mimic both bacterial and mammalian cells depending on the lipid composition employed. Because of this, the assay

solution, and the catalytic center is activated. Glucose is then oxidized to glucono lactone, reducing PQQ through a two-electron exchange. The reduced PQQ in turn reduces the redox dye DCPIP, which changes color from blue in its oxidized form to colorless in its reduced form (Figure 8). The optical absorbance

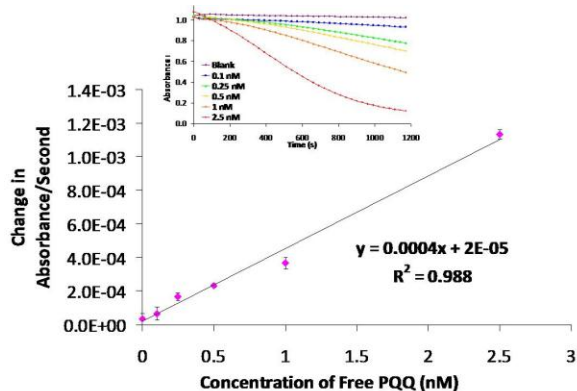


Figure 9: Dose response of free PQQ in optical assay. PQQ concentrations are 0.1nM, 0.25nM, 0.5nM, 1nM, 2.5nM.

can be tailored to determine the antimicrobial activity of peptides and copolymers against both gram positive and gram negative bacteria, as well as the hemolytic activity against human cells.

The model antimicrobial peptides used in this study are MSI-594 and MSI-78, whose sequences can be found in Table 1. The mechanisms for membrane permeabilization have been described by

PEPTIDE	SEQUENCE
MSI-594	GIGKFLKKAKKIGAVLKVLTTGL-NH ₂
MSI-78	GIGKFLKKAKKFGKAFVKILKK-NH ₂
rIAPP	KCNTATCATQRLANFLVRSSNNLGPVLPPTNVGSNTY-NH ₂

Ramamoorthy et al. elsewhere²⁷. The ability of these peptides to permeabilize membranes is

Table 2: Copolymer structure and degree of alkylation

Polymer	R	f_{alkyl}
P ₀	–	0.00
PB ₂₀	Butyl	0.20
PB ₃₆	Butyl	0.36
PB ₅₄	Butyl	0.54
PB ₇₉	Butyl	0.79
PH ₁₈	Hexyl	0.18
PH ₃₃	Hexyl	0.33
PH ₅₁	Hexyl	0.51
PH ₆₃	Hexyl	0.63

compared to a control peptide, rat islet amyloid polypeptide (rIAPP), which binds to phospholipid membranes without disrupting most membrane compositions²⁸⁻²⁹. Along with these peptides, the study focused on two series of methacrylamide copolymers,

the PB and PH series (see Figure 2). Within each series, polymers with varied alkyl side chain lengths were tested as well (Table 2).

In this work, PQQ-loaded liposomes are incubated with an antimicrobial peptide (MSI-594 or MSI-78), the control peptide, or a methacrylamide copolymer. Incubation with the antimicrobial peptide or copolymer results in the lysis of the liposome membrane, resulting in the release of the encapsulated PQQ. In the absence of peptide, or during incubation with the control rIAPP, the liposome membrane is not compromised and no PQQ is released. The release of free PQQ is monitored by an optical absorbance assay that measures the color change due to the reduction of DCPIP (Figure 8). The peptide and polymer activities are measured continuously for kinetic studies, as well as through a fixed endpoint assay to determine total

activity. The resulting antimicrobial activity of the peptides is compared to the results of liposomes loaded with a fluorescent dye, while the antimicrobial and hemolytic activity of the copolymers are compared to the literature values provided by Kuroda et al.

Next, the development of a novel technique for HIT diagnosis combining the colorimetric PQQ assay and complement fixation is discussed, taking advantage of the sensitivity afforded by the PQQ assay as well as the selectivity

of complement fixation. Ideally, this would involve the immobilization of PF4 onto the liposome surface, followed by the addition of heparin to form heparin-PF4 complexes on the

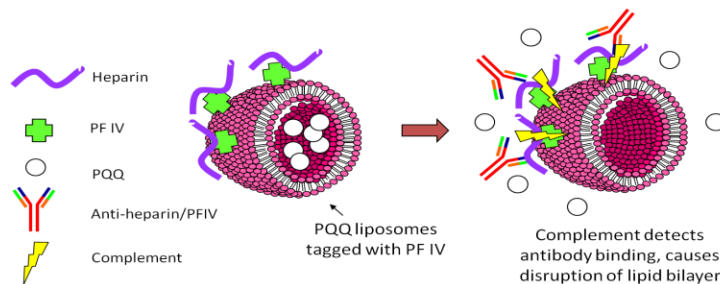


Figure 10: HIT diagnostic assay concept. Immobilizing PF4 on the liposome surface would allow the heparin and anti-heparin complex to form on the surface, resulting in lysis in the presence of complement.

surface of the liposomes (Figure 10). In the presence of the anti-heparin-PF4 IgG antibodies, the addition of complement would cause membrane lysis and result in a positive test; without target antibodies present, the addition of complement should not cause lysis. This lysis will be detected by the reduction of DCPIP, and subsequent color change.

Initially, a model system employing liposomes with a 2,4-dinitrophenyl (DNP) containing lipid is used. The DNP molecules on the outer surface of the liposome act like the heparin-PF4 complex on the surface of the liposomes (for the purpose of testing feasibility), which complexes to anti-DNP antibodies in solution. Complement will then bind to the DNP/anti-DNP complexes and disrupt the lipid membrane, resulting in liposome lysis. The addition of complement without anti-DNP present should not cause liposome lysis. Preliminary progress on this new research project is reported, including the characterization of the liposomes and attempted proof-of-concept experiments.

MATERIALS AND METHODS

Materials

PQQ was purchased from Berry & Associates (Dexter, MI). PQQ-dependent apo-glucose dehydrogenase, 2-[4-(2-hydroxyethyl)-1-piperazine]ethanesulfonic acid (HEPES), and sodium azide were obtained from Fisher Scientific (Pittsburgh, PA). L- α -Phosphatidylcholine (egg PC), 1-palmitoyl-2-oleoyl-*sn*-glycero-3-phosphoethanolamine (POPE), 1-palmitoyl-2-oleoyl-*sn*-glycero-3-phospho-(1'-*sn*-glycerol) (POPG), 1,2-dioleoyl-*sn*-glycero-3-phosphate (DOPA), 1,2-dioleoyl-*sn*-glycero-3-phospho-(1'-*rac*-glycerol) (DOPG), 1,2-dioleoyl-*sn*-glycero-3-[phospho-*rac*-(3-lysyl(1-glycerol))] (lysyl-DOPG), 1,1'2,2'-tetraoleoyl cardiolipin (CL), 1,2-dipalmitoyl-*sn*-glycero-3-phosphoethanolamine-N-(2,4-dinitrophenyl) (DNP PE), and 1,2-dipalmitoyl-*sn*-glycero-3-phosphoethanolamine-N-[6-[(2,4-dinitrophenyl)amino]hexanoyl] (DNP cap PE) were purchased from Avanti Polar Lipids (Alabaster, AL). Model peptides MSI-594 and MSI-78 were synthesized as described elsewhere²⁷. Rat islet amyloid polypeptide (rIAPP) was a product of AnaSpec (Fremont, CA). The PH and PB series copolymers were synthesized as described elsewhere⁶. Cholesterol, sodium chloride, calcium chloride, and glucose were obtained from Sigma-Aldrich (St. Louis, MO), as were anti-DNP monoclonal antibodies, complement from human serum, and guinea pig complement sera. All the solutions/buffers used in this work were prepared in the laboratory using Milli-Q grade deionized water (18.2 M Ω , Millipore Corp., Billerica, MA). All experiments were performed in triplicate at room temperature.

Instrumentation

A MTX Laboratory Systems Inc. (Vienna, VA) 96-well microtiter plate reader was used to monitor the activity of the glucose dehydrogenase enzyme after reconstitution with PQQ

released from the liposomes. The instrument utilized a 595 nm filter to record the optical absorbance of the test solution as a function of time for kinetic studies. For the endpoint assay, an initial measurement was recorded before the addition of glucose. Glucose was added and the plate was allowed to sit for 30 min. After 30 min, a final absorbance measurement was made. The difference in absorbance between the two measurements was related to the peptide or polymer activity.

Preparation of PQQ-loaded Liposomes

Unilamellar liposomes were prepared using the freeze/thaw method followed by extrusion³⁰. Lipids dissolved in chloroform were combined in a glass tube. The chloroform was then evaporated using a rotary evaporator, resulting in a dried lipid film on the interior of the glass tube. This step was repeated after re-dissolving the lipids in chloroform. The lipid film was re-dried under vacuum for 1 h. The film was resuspended in a 250 μ M PQQ solution in HEPES buffer (working buffer: 20 mM, pH 7.0, 290 mOsmol/kg). The liposomes underwent five freeze/thaw cycles in super-cooled ethanol, after which they were extruded through a 0.22 μ m polycarbonate filter four times. Finally, the liposomes were separated from any remaining free PQQ with a Sephadex G-50 medium-grade size exclusion column.

Optimization of Human Cell Mimic Liposome Composition

Liposomes composed of four different lipid compositions were prepared. For direct analysis, all the liposomes were diluted to the same lipid concentration (3.18 mM). The liposomes were incubated with the model peptide MSI-594 for 30 min. After incubation, a 5 μ L aliquot of the reaction mixture were tested in a PQQ assay containing 25 μ L 50 μ g/mL apo-

GDH, 25 μL 80 mM glucose, 30 μL 0.5 mM DCPIP, and working buffer to bring the total volume to 100 μL . Absorbance measurements were taken at 595 nm every 30 s for a total assay time of 19 min 30 s.

Liposome Characterization

Liposome concentration was determined using the Bartlett phosphate assay³¹. The average liposome size was determined through dynamic light scattering (DLS) on a Nicomp 380 ZLS Particle Sizing System (Santa Barbara, CA). The results of the phosphate assay and light scattering experiments were used to estimate the number of liposomes per unit volume. The average diameter determined by DLS was used to estimate the liposome surface area, and the average head group surface area was assumed to be 60 \AA^2 . Therefore, for a given liposome size and phosphate concentration, the number of liposomes per unit volume can be calculated.

To calculate the average amount of encapsulated PQQ, a PQQ assay using a dilute solution of liposomes lysed with Tween-20 surfactant was employed. The PQQ released from this assay was compared to a calibration curve of free PQQ. Five μL of diluted liposomes were tested in an assay containing 5 μL 50 $\mu\text{g}/\text{mL}$ apo-GDH, 7.5 μL 20mM calcium chloride, 25 μL 80 mM glucose, 30 μL 0.5 mM DCPIP, and 10 μL 10% (wt/wt) Tween-20. The assay was brought to 100 μL volume using working buffer. The determined number of PQQ molecules was divided by the number of liposomes in the assay, resulting in an estimated number of PQQ molecules per liposome.

The stability of liposomes stored at 4°C was determined by a PQQ assay run with liposomes, both with and without the presence of Tween-20 surfactant, without the addition of calcium. An initial stability was determined immediately after preparation and compared to

stability assays run each following week. Five μL of liposomes were tested in an assay containing 5 μL 500 $\mu\text{g}/\text{mL}$ apo-GDH, 25 μL 80 mM glucose, 30 μL 0.5 mM DCPIP, and 10 μL 10% (wt/wt) Tween-20. The assay was brought to 100 μL volume using working buffer. The absorbance of the reaction was monitored at 595 nm every 30 s for a total assay time of 19 min 30 s. Any response in the absence of Tween-20 was due to the presence of free PQQ outside the liposome shell, indicating a loss of liposome integrity.

Optimization of Liposome Concentration for Assay Detection

Various liposome concentrations were incubated in solution with a final concentration of 4 μM MSI-594 peptide for 30 min. After incubation, a 5 μL aliquot of the reaction mixture was tested in a PQQ assay containing 25 μL 50 $\mu\text{g}/\text{mL}$ apo-GDH, 25 μL 80 mM glucose, 30 μL 0.5 mM DCPIP, and working buffer to bring the total volume to 100 μL . Absorbance measurements were taken at 595 nm every 30 s for a total assay time of 19 min 30 s.

Evaluation of Antimicrobial Peptide Activity

Comparison with Non-Permeabilizing Peptide

Liposomes at a total lipid concentration of 0.4 mM were added to the wells of a 96 well microtiter plate. The antimicrobial or a control peptide was added in varying concentrations. Also added were 5 μL 500 $\mu\text{g}/\text{mL}$ apo-GDH, 30 μL 0.5 mM DCPIP, 25 μL 80 mM glucose, and working buffer to bring the total volume to 100 μL . The absorbance was measured 40 times at 595 nm every 30 s, for a total assay time of 19 min 30 s. In between measurements, the plate was shaken to ensure complete mixing of the assay reagents. These experiments were conducted

using two liposome compositions – a 1:1:1 mole ratio of egg PC:DOPA:cholesterol and a 3:1 mole ratio of egg PC:POPG.

Endpoint Assay for Peptide Activity

For the endpoint assay of MSI-594, the microtiter plate was prepared in the manner described above. Before the addition of glucose, however, an initial absorbance measurement was taken. The same concentration of glucose as described above was added, and plate was allowed to sit for 30 min. At the end of 30 min, a final absorbance measurement was recorded. The absorbance difference between the measurements was then related to the activity of the peptide. These experiments were only conducted using the 3:1 mole ratio of egg PC:POPG liposomes.

Comparison to Fluorescent Dye-Loaded Liposomes

Unilamellar liposomes consisting of a 1:1:1 mole ratio of egg PC:DOPA:cholesterol were prepared as described above using the fluorescent dye 8-hydroxypyrene-1,3,6,-trisulfonic acid (HPTS) instead of PQQ. Liposomes at a total lipid concentration of 0.4 mM were added to a plastic cuvette. Various concentrations of MSI-594 were added to the cuvette, and the resulting fluorescent signal was measured using a fluorimeter (Shimadzu; Columbia, MD), with an excitation wavelength of 413 nm and an emission wavelength of 510 nm.

Evaluation of Synthetic Copolymer Activity

Effects of Hydrophobicity on Activity

The two series of copolymers, PH and PB, each with varying fractions of side chain alkylation, were analyzed for membrane permeabilization activity. The polymers were initially dissolved in dimethyl-sulfoxide to create 1 mg/mL solutions, which were further diluted in the assay. Liposomes, at a total lipid concentration of 0.4 mM, were added to the wells of a 96 well microtiter plate. Each of the copolymers were added to the wells at a final concentration of 5 μ g/mL, followed by 5 μ L of 500 μ g/mL of apo-GDH, 30 μ L 0.5 mM DCPIP, 25 μ L 80 mM glucose, and working buffer to bring the total volume to 100 μ L. The absorbance was measured 40 times at 595 nm every 45 s for a total assay time of 29 min 15 s, shaking the plate in between measurements to ensure complete mixing of the assay reagents. These experiments were conducted using two liposome compositions – a 1:1:1 mole ratio of egg PC:DOPA:cholesterol and a 4:1 mole ratio of POPE:POPG.

The limits of the detection for this system were determined by evaluating the dose-responses of the most active polymers from the PH and PB series based on the lipid composition for egg PC, DOPA, and cholesterol liposomes, PH₅₁ and PB₅₄. The polymers were added to the assay in concentrations ranging from 0.5 – 4 μ g/mL. The remaining reagents were added as described above. The absorbance was measured 40 times at 595 nm every 45 s for a total assay time of 29 min 15 s, shaking the plate in between measurements to ensure complete mixing of the assay reagents.

Endpoint Assay for Polymer Activity

For the endpoint assay of the copolymers, the most active polymers of the PH and PB series based on the two liposome compositions were used. For the POPE/POPG liposomes, PH₅₁

and PB₂₀ were used. For the egg PC/DOPA/ cholesterol liposomes, PH₅₁ and PB₅₄ were used. The microtiter plate was prepared in the manner described above. Before the addition of glucose, however, an initial absorbance measurement was taken. The same concentration of glucose as described above was added, and the plate was allowed to sit for 30 min. At the end of 30 min, a final absorbance measurement was recorded. The absorbance difference between the measurements was then related to the activity of the polymers.

Evaluation of Assay Using Gram-Positive Bacteria Liposome Mimics

Unilamellar liposomes consisting of a 12:7:1 mole ratio of DOPG/lysyl-DOPG/cardiolipin (CL) were prepared as described above. Liposomes at a total lipid concentration of 0.4 mM were added to the wells of a 96 well microtiter plate. The peptides MSI-78 and MSI-594 and the polymers PH₅₁ and PB₂₀ were added to the microtiter plate at a final concentration of 5 μ M. The remaining reagents were added as described above. The absorbance was measured 40 times at 595 nm every 45 s for a total assay time of 29 min 15 s, shaking the plate in between measurements to ensure complete mixing of the assay reagents.

Evaluation of DNP Model System

Optimization of DNP Liposomes Lipid Composition

Four lipid compositions were attempted for the development of the DNP model system for complement fixation detection. Three of the compositions consisted of varying mole ratios of egg PC, DOPA, cholesterol, and DNP PE, while the fourth employed DNP cap PE as the DNP-containing lipid. Liposome concentration was determined using the Bartlett phosphate assay.

The stability of these liposomes, as well as the average number of encapsulated PQQ molecules, was determined as described above. The viability of the composition for the DNP model system was tested using both the competitive binding and the complement fixation-based PQQ assays described below.

UV-visible Absorbance of DNP Liposomes

To determine whether or not DNP molecules were present on the surface of liposomes, UV-visible absorbance spectra were taken for 1:1:1 mole ratio egg PC:DOPA:cholesterol liposomes and 33:33:33:1 mole percent egg PC:DOPA:cholesterol:DNP PE liposomes using a spectrophotometer (Shimadzu; Columbia, MD). Liposomes at a total lipid concentration of 0.4 mM were added to a plastic cuvette in working buffer. The spectra were obtained at wavelength intervals of 1 nm from 250 nm to 600 nm, using working buffer as a blank.

Competitive Binding Assay

To determine that DNP molecules present on the liposome surface can actually bind to the anti-DNP antibody, an adaption of the competitive binding assay based on a biotin-avidin model system²⁵ was used. The anti-DNP antibody was reacted with the surface of pre-activated NUNC amino microtiter plate wells (Fisher Scientific; Pittsburgh, PA) by adding 5 μ L of 1.1 mg/mL anti-DNP and 95 μ L of 100 mM sodium carbonate buffer (pH 9.6, conjugation buffer) to the wells for 90 min. After the wells were washed with carbonate buffer, 150 μ L of 40 mM ethanolamine were added to the wells for 1 h to cap any un-reacted sites on the surface of the plates. The plates were then washed three times with carbonate buffer, and subsequently rinsed one time each with Tris buffer and HEPES working buffer to remove any un-reacted anti-DNP.

Thirty μL of either 1nM 33:33:33:1 mole percent egg PC:DOPA:cholesterol:DNP PE liposomes or 1:1:1 mole ratio egg PC:DOPA:cholesterol liposomes and 70 μL working buffer were added to control wells without anti-DNP in addition to wells that had been reacted with anti-DNP. The liposomes were allowed to incubate in the microtiter plate for 45 min. After incubation, the wells were washed twice with working buffer before the addition of 5 μL 500 $\mu\text{g}/\text{mL}$ apo-GDH, 25 μL 80 mM glucose, 30 μL 0.5 mM DCPIP, and 10 μL 10% (wt/wt) Tween-20 (to lyse any bound liposomes). The assay was brought to 100 μL volume using working buffer. The absorbance of the reaction was measured 40 times at 595 nm every 60 s for a total assay time of 39 min, shaking the plate in between measurements to ensure complete mixing of the assay reagents.

PQQ-Based Liposome Assay of Complement Fixation

The complement fixation assay based on PQQ loaded liposomes was developed to contain three controls as well as the complement fixation assay. The controls were comprised of liposomes, liposomes with anti-DNP, and liposomes with complement. The assay included liposomes, anti-DNP, and complement. Along with the DNP linked-liposomes described above, liposomes composed of egg PC, DOPA, and cholesterol that did not contain DNP PE were tested in the assay as a non-reactive control. All of the parameters except liposome concentration, which was fixed at a total lipid concentration of 0.72 mM, were varied throughout the development of the assay. The anti-DNP concentration ranged from a final concentration of 17 – 250 ng/mL. The amount of complement ranged from a final concentration of 100 ng/mL to 2.5 $\mu\text{g}/\text{mL}$, with complement prepared from both guinea pig and human sera being used. The assay was incubated prior to the addition of complement for times varying from no incubation to 1 h.

After incubation, 5 μL 500 $\mu\text{g}/\text{mL}$ apo-GDH, 25 μL 80 mM glucose, and 30 μL 0.5 mM DCPIP were added to the microtiter plate, with working buffer added to bring the total volume to 100 μL . The absorbance was measured 40 times at 595 nm either every 45 s or every 60 s for a total assay time of 29 min 15 s or 39 min, respectively, shaking the plate in between measurements to ensure complete mixing of the assay reagents.

RESULTS AND DISCUSSION

GDH-PQQ Reconstitution Assay

The PQQ reconstitution assay has been previously described^{25,32}. In this assay, free PQQ is released from the liposomes after membrane permeabilization, resulting in the activation of apo-GDH. After activation, PQQ becomes a catalytic center where glucose is oxidized into glucono

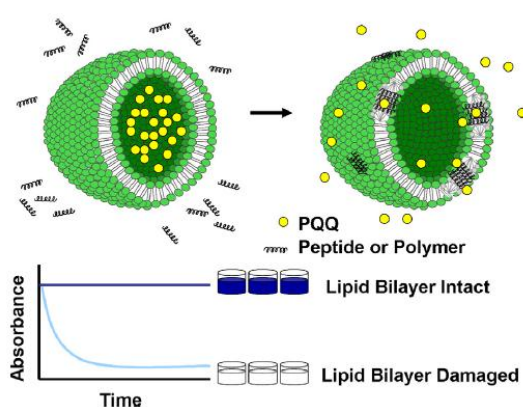


Figure 11: Assay concept. In the presence of a membrane-permeabilizing agent, a color change proportional to the concentration of peptide or copolymer in solution occurs.

lactone, resulting in a two-electron transfer that reduces PQQ. At this point, the redox dye DCPIP is reduced by PQQ, resulting in a color change from dark blue to colorless (Figure 11). It should be noted that calcium was not added to the assay, as it has been shown that the presence of calcium facilitates the disruption of lipid membranes, generating a false positive signal for membrane disruption^{33,34}. This does result in a decrease in GDH activity, but, due to the homogeneous nature of the assay, does not completely eliminate it, with small concentrations of PQQ still resulting in quick and substantial changes in absorbance signal. Because of the optical nature of the assay, it is advantageous in that it can yield a clear visual change in a short amount of time. Furthermore, no expensive or complicated instrumentation is required to detect a clear positive response for a species that increases membrane permeabilization.

Optimization of Human Cell Mimic Liposome Composition

The results of the optimization of a liposome composition are shown in Figure 12. The human cell mimics were based on the composition of human erythrocyte membranes, which are composed mainly of proteins and lipids, specifically cholesterol and phospholipids³⁵. One of the major phospholipids present in these membranes is phosphatidylcholine (PC). Because of this, each of the four compositions tested contained PC.

When tested with model peptide MSI-594, it was observed that liposomes composed entirely of PC showed a good response to this peptide. Liposomes composed of a 1:1 mole ratio of PC:DOPA, on the other hand, showed no response. However, the addition of cholesterol to liposomes containing PC and DOPA resulted in an excellent response to the peptide. Because

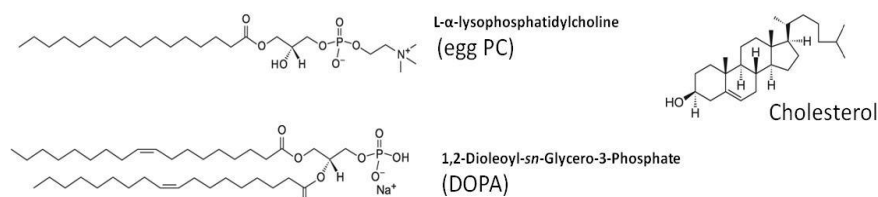


Figure 13: Lipid structures for egg PC, DOPA, and cholesterol.

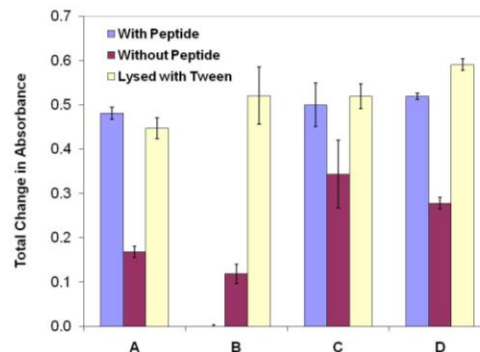


Figure 12: Liposome composition optimization. Liposome response to MSI-594 for A) egg PC only liposomes, B) 1:1 mole ratio egg PC:DOPA liposomes, C) 4:4:1 mole ratio egg PC:DOPA:cholesterol liposomes, and D) 1:1:1 mole ratio egg PC:DOPA: cholesterol liposomes

the addition of cholesterol stabilizes the lipid membrane, and because cholesterol

is known to be present in human cells, the liposome composition consisting of a 1:1:1 mole ratio of PC:DOPA:cholesterol was used for all further human cell mimic testing (Figure 13).

Table 3: Liposome Characterization

Average Size (nm)	151 ± 26
Average number of PQQ molecules	15 ± 5
Stability	> 3 weeks at 20°C

Liposome Characterization

Liposomes composed of a 1:1:1 mole ratio of PC:DOPA:cholesterol were used for the

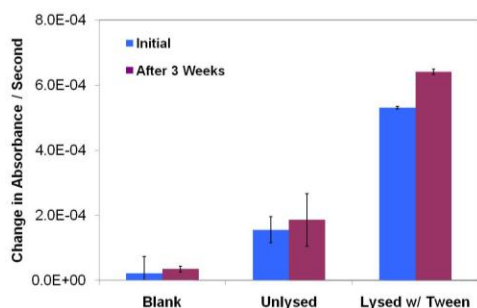


Figure 14: Stability of egg PC, DOPA, and cholesterol liposomes. After three weeks of refrigerated storage, there is no significant signal change in unlysed liposomes, suggesting the lipid membrane is still intact.

Liposome stability and PQQ-encapsulation data were obtained by running the reconstitution assay with liposomes in presence and absence of the detergent Tween-20. In the presence of Tween-20, the lipid membrane is completely and irreparably destroyed, resulting in the release of all the encapsulated PQQ. Because the PQQ released can be

determination of general liposome characteristics (Table 3). These liposomes were shown to be stable for at least three weeks when stored in the refrigerator (Figure 14). The PQQ-loaded liposomes were determined to be approximately 150 nm in diameter (Figure 15), containing roughly 15 molecules of PQQ per liposome.

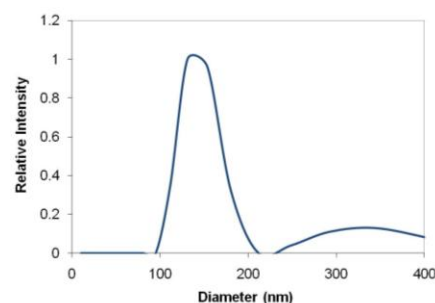


Figure 15: Average liposome size. Liposomes are approximately 150 nm in diameter.

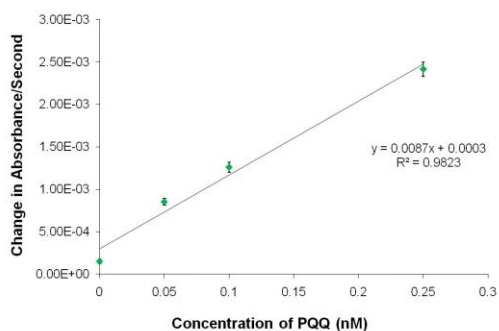


Figure 16: Free PQQ calibration curve. PQQ concentrations range from 0.05nM to 0.25nM. Used to determine total PQQ encapsulation.

quantified, the number of PQQ molecules present in the assay can be calculated using a calibration curve (Figure 16). In the absence of Tween-20 or a permeabilizing agent (such as peptide or polymer), the lipid membrane should remain intact. If a signal is detected in the absence of Tween-20, it suggests the

integrity of the lipid membrane has been compromised, which can be indicative of the degradation of liposome stability over time. Therefore, the liposomes were considered to be stable if no significant signal was observed in the absence of detergent. As can be seen in Figure 14, the liposomes do not show substantial leakage over a three week period, suggesting their good stability over this time period.

The amount of encapsulated PQQ reported in Table 3 is much lower than would be expected using a 250 μM PQQ solution during liposome preparation. The theoretical maximum encapsulation is calculated using the average liposome interior radius of 1×10^{-5} cm and the equation for the volume of a sphere, resulting in an interior volume of 4.19 attoliters. Based on this volume, the maximum number of PQQ molecules that can be encapsulated is approximately 630. The observed PQQ encapsulation then is approximately 2% of the theoretical encapsulation efficiency. This low observed encapsulation of PQQ could be due to electrostatic repulsions between PQQ molecules and the lipid membrane. At neutral pH, PQQ has three negative charges present on each molecule. The liposomes are also highly negatively charged due to the presence of DOPA lipids, each of which has a negative charge on the hydrophilic head group (Figure 13). The repulsions between the negatively charged PQQ and the DOPA head groups could reduce the encapsulation efficiency of the liposomes.

Optimization of Liposome Concentration for Assay Detection

To determine the optimal liposome concentration for use in the assay, the concentration of egg PC, DOPA, and cholesterol liposomes was varied from 1 nM to 30 nM (initial concentration) and the assay was performed using a high concentration (16 μM) of MSI-594 (Figure 17). The greatest response to peptide was observed when the liposome concentration

was between 0.4 mM total lipid and 1 mM total lipid. Therefore, liposomes were used at a lipid concentration of 0.4 mM (corresponding to an initial concentration of 1 nM liposomes) for all subsequent experiments.

Evaluation of Antimicrobial Peptide Activity

Comparison with Non-Permeabilizing Peptide

Peptide activity was tested using two different liposome compositions. The first composition, a 3:1 mole ratio of egg PC:POPG, was used as a bacterial cell mimic to determine

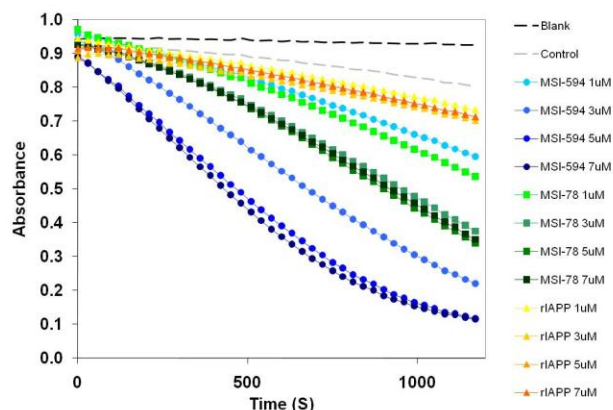


Figure 18: Antimicrobial dose response for MSI-594 and MSI-78, compared to rIAPP. Peptide concentrations were 1 μ M, 3 μ M, 5 μ M, and 7 μ M. The assay selectivity over rIAPP is demonstrated.

the antimicrobial activity of peptides. The activity of two model peptides, MSI-594 and MSI-78, was tested using these PC:POPG liposomes. In order to establish their relative activities, they were compared to the inactive control peptide rIAPP. The concentrations of these peptides were varied from 1-7 μ M, and their membrane permeating ability was monitored through a 20 min kinetic absorbance assay (Figure 18). The relative membrane permeabilization rates can be seen, with MSI-594 permeating at a higher rate than MSI-78 and rIAPP exhibiting a signal barely higher than that of liposomes in the absence of any peptide.

In order to compare the antimicrobial activity of these peptides, the change in absorbance per second of each peptide was plotted (Figure 19). Due to a varied assay response between

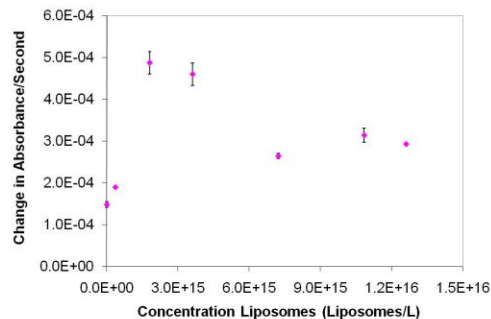


Figure 17: Liposome concentration optimization. Liposomes ranging in concentration from 1 nM to 30 nM were tested with a high concentration (16 μ M) of MSI-594. The liposome concentration range showing highest response was from 5 nM to 10 nM.

the antimicrobial activity of peptides. The activity of two model peptides, MSI-594 and MSI-78, was tested using these PC:POPG liposomes. In order to establish their relative activities, they were compared to the inactive control peptide rIAPP. The concentrations of these peptides were varied from 1-7 μ M, and their membrane permeating ability was

liposome batches (based on variances in PQQ encapsulation efficiency), the assay signal for this data was normalized based on making the change in absorbance per second for PQQ release of liposomes incubated with 7 μM MSI-594 equal to 100% of the total observed slope. The absorbance change for the remaining peptides and concentrations was taken as a fraction of this total slope. As can be seen in Figure 19, the active MSI-594 and MSI-78 peptides show a significant increased response over the inactive rIAPP peptide, demonstrating the selectivity of the method for membrane-permeabilizing peptides over inert peptides. The ability to select for peptides with permeating antimicrobial activity displays the technique's capability for peptide screening.

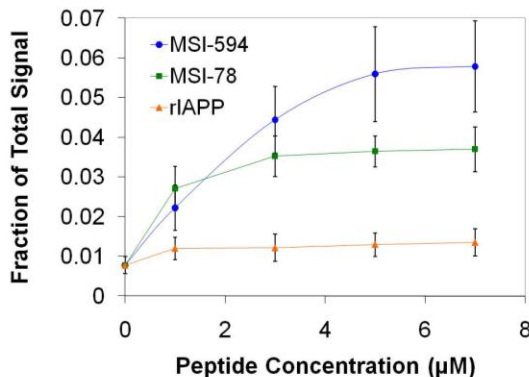


Figure 19: Normalized response of assay to varied concentrations of MSI-594, MSI-78, and rIAPP (n=3). The response was normalized by taking the change in absorbance/sec of 7 μM MSI-594 as 100% of the total observed slope, with each other measurement take

Furthermore, it can be seen that both active peptides are capable of permeating membranes to the same extent as Tween-20. The difference in signal observed between the two active peptides MSI-594 and MSI-78 is related to differences in their membrane-permeating mechanisms²⁷. Therefore, it can be seen that although both peptides demonstrate strong antimicrobial activity, MSI-594 permeates membranes at a faster rate than does MSI-78,

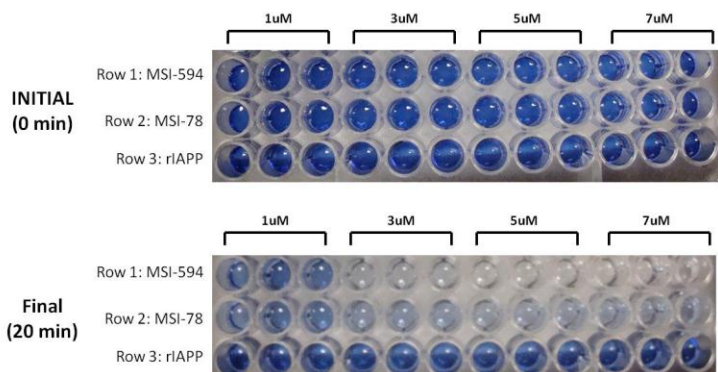


Figure 20: Visual change of varying concentrations of MSI-594 and MSI-78 compared to control peptide rIAPP before and after 20 min assay.

especially at higher concentrations of peptide.

Images of the microtiter plate before and after the completion of the kinetic assay are shown in Figure 20.

It can be seen that wells containing the

permeabilizing peptides MSI-594 and MSI-78 were colorless at the end of the 20 min assay, while those wells containing the inactive rIAPP were still dark blue. This demonstrates the visual nature of the assay, as positive identification of membrane lysis can be determined without the use of instrumentation.

Liposomes composed of a 1:1:1 mole ratio of egg PC:DOPA:cholesterol were used as

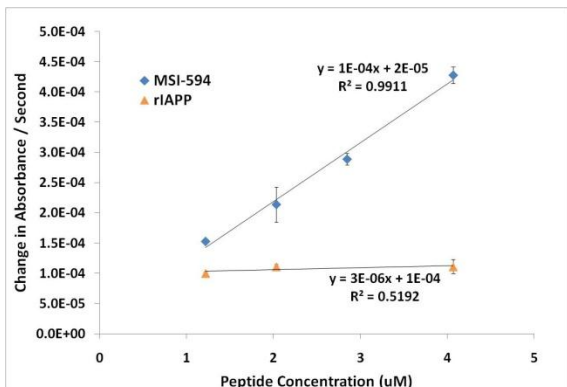


Figure 21: Hemolytic dose response of MSI-594 compared to rIAPP. Assay selectivity over the control peptide is demonstrated.

compared to equivalent concentrations of rIAPP. The MSI-78 data in Figure 22 is normalized using the same process as before, taking the change in absorbance per second for PQQ release of liposomes incubated with 12.11 μ M MSI-78 as equal to 100% of the total observed slope. The MSI-594 data is not normalized. It can be seen that the MSI-594 and MSI-78 peptides continue to demonstrate higher rates of activity over the inactive rIAPP, suggesting that the assay can also be used to determine the activity, and therefore the toxicity, of peptides against human cells.

Endpoint Assay for Peptide Activity

human cell mimics to demonstrate the assay's validity in monitoring the potential toxicity of antimicrobial peptides towards human cells. As the more active peptide, the concentration of MSI-594 was varied from 1.22-4.07 μ M (Figure 21), while the MSI-78 concentrations were varied from 6.06-

12.11 μ M (Figure 22). Both peptides were

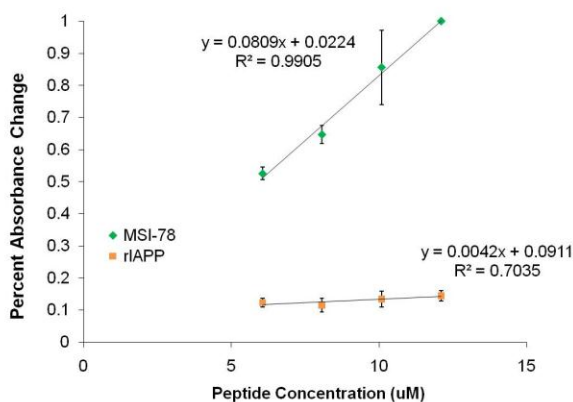


Figure 22: Hemolytic dose response for MSI-78 versus rIAPP. Assay selectivity over the control peptide is demonstrated.

To demonstrate the applicability of this system as a visual method for simple positive or negative membrane permeabilization detection, an endpoint assay was applied using MSI-594.

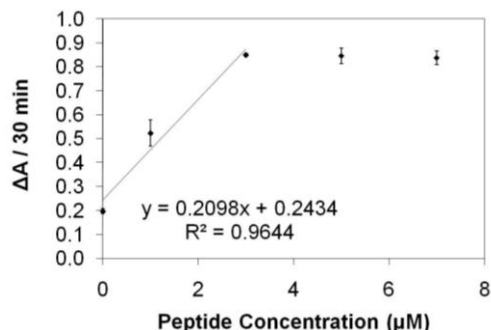


Figure 23: Endpoint assay for determination of the antimicrobial activity of MSI-594. The detection limit for this system was determined to be 396nM.

this endpoint detection method, MSI-594 can be detected at micro-molar levels. The limit of

detection for this method, defined as the concentration of peptide equivalent to the absorbance change of three times the standard deviation of the control, was determined to be 396 nM. This limit of

detection is comparable to reported values

of liposome-based methods of MSI-594 detection that use fluorophores as the encapsulated tracer molecule²⁷. Furthermore, the detection range of this method is analogous to related

experiments performed using liposomes encapsulating the fluorescent dye HPTS (Figure 25), which is a molecule similar in size and charge to PQQ. In these experiments, HPTS-encapsulated liposomes were combined with varied concentrations of MSI-594, ranging from 0.2-2.0

In this assay, an initial absorbance measurement was recorded, and a final absorbance was measured 30 min later (Figure 23). The overall visual nature of this assay is shown in Figure 24. Once again, it can be seen that wells containing MSI-594 are visually distinguishable from those that do not, which are still dark blue. Using

this endpoint detection method, MSI-594 can be detected at micro-molar levels. The limit of

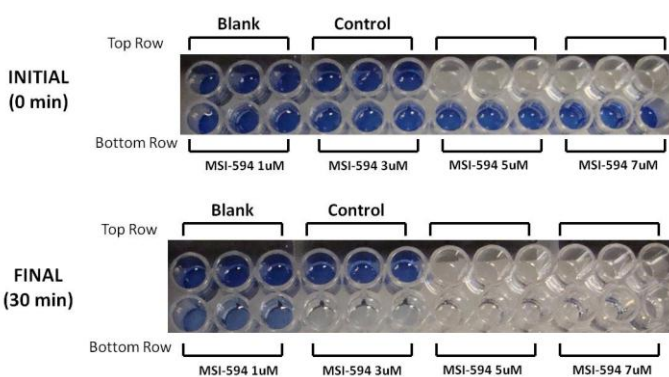


Figure 24: Visual detection of MSI-594 antimicrobial activity before and after 30min endpoint assay.

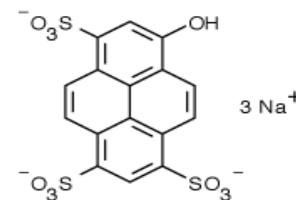


Figure 25: Structure of fluorescent dye HPTS.

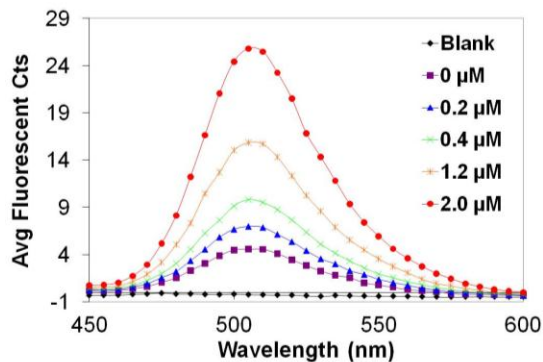


Figure 26: Detection of varied MSI-594 concentrations using liposomes encapsulating the fluorescent dye HPTS. Excitation wavelength: 413 nm. Emission wavelength: 510 nm.

μM , in a plastic cuvette, and the resulting fluorescence was monitored (Figure 26). The ability to visually detect low levels of antimicrobial peptides without instrumentation by using the PQQ loaded liposomes in place of fluorophores allows this system to be a useful method for the simple and relatively quick screening of peptide activity.

Evaluation of Synthetic Copolymer Membrane Permeabilizing Activity

Effects of Hydrophobicity on Activity

The assay system was used to test the antimicrobial and hemolytic activity of two copolymer series, PH and PB, both with varying degrees of side chain alkylation ranging from 0 (zero hydrophobicity) to 80 (Table 1). Antimicrobial activity was monitored using *E. coli* cell

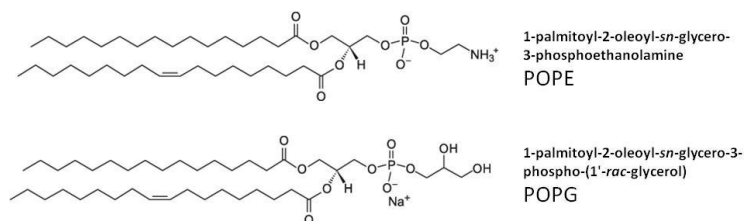


Figure 27: Lipid structures of POPE and POPG.

mimics, liposomes composed of a 4:1 mole ratio of POPE:POPG (Figure 27), while the potential toxicity towards human cells

(hemolytic activity) was determined using 1:1:1 mole ratio egg PC:DOPA:cholesterol liposomes as human cell mimics.

Assay results were compared to previously described membrane disruption activities⁷, where it has been demonstrated that the PH series is more active overall than the PB series. The reported antimicrobial activity of the PH series shows an initial decrease in activity as f_{alkyl}

increased from 0.00-0.33. However, as f_{alkyl} increased towards 0.63, the activity increases with overall faster kinetic responses. For the PB series, activity is sharply decreased as f_{alkyl} increases from 0.00-0.54, followed by a large change in kinetic response as f_{alkyl} is increased to 0.79.

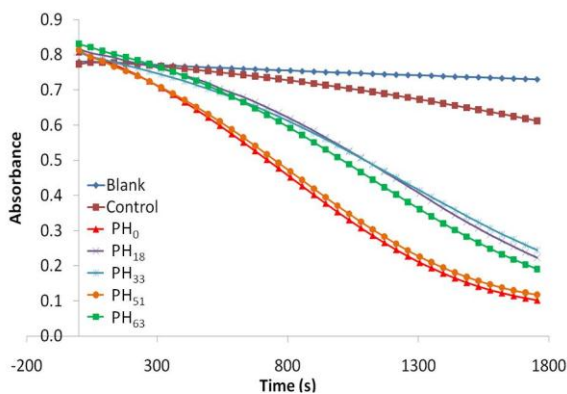


Figure 28: Kinetic assay for antimicrobial activity for PH series with varied degrees of alkylation.

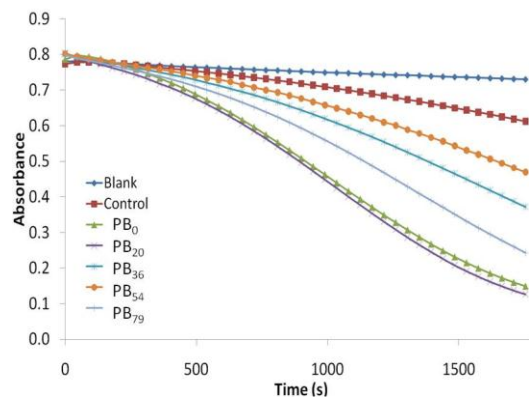


Figure 29: Kinetic assay for antimicrobial activity for PB series with varied degrees of alkylation.

In order to test the relative antimicrobial activity for each degree of alkylation in both series, 5 $\mu\text{g/mL}$ of each polymer were incubated with POPE/POPG liposomes, and the activity was monitored via a 29 min kinetic absorbance assay (Figures 28-29). Comparing these two

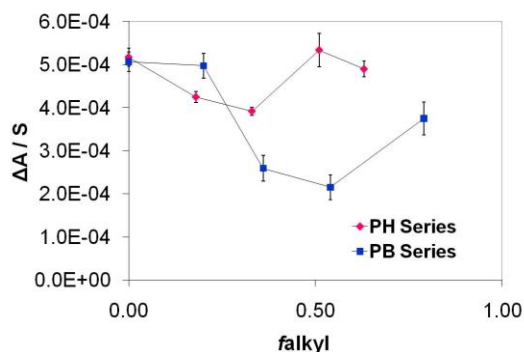


Figure 30: Comparison of kinetic response of antimicrobial activity of the PH and PB series with varying f_{alkyl} values ($n=3$).

figures, it can be seen that the PH series appears to be, on the whole, more active than the PB series. A direct comparison of the two series can be seen in Figure 30. As shown in this figure, the antimicrobial activity of the PH series decreases as f_{alkyl} moves from 0.00 to 0.33, and then increases towards 0.63.

The antimicrobial activity of the PB series decreases initially as f_{alkyl} climbs to 0.54, but increases with f_{alkyl} after that. The observed antimicrobial activity of these two series follows that reported in the literature⁷, demonstrating the ability of the

method to not only screen for antimicrobial activity, but to determine the relative activity of antimicrobial agents.

Similarly, to test the polymer series for potential hemolytic toxicity, 5 $\mu\text{g/mL}$ of each polymer were incubated with egg PC, DOPA, and cholesterol liposomes, and the activity was

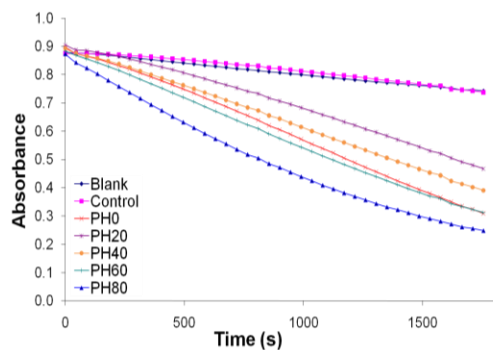


Figure 31: Kinetic assay for hemolytic activity for PH series with varied degrees of alkylation.

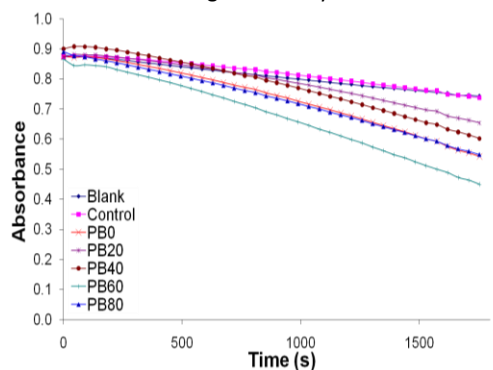


Figure 32: Kinetic assay for hemolytic activity for PB series with varied degrees of alkylation.

PH series. The PB series, on the other hand, shows fairly steady hemolytic activity, with a slight initial decrease followed by a slight increase in activity. While the PH series continues to show high membrane permeabilizing activity for the cholesterol-containing human cell mimics, demonstrating little selectivity for bacterial cell mimics without cholesterol, the PB series

monitored through a 29 min kinetic absorbance assay (Figures 31-32). As reported for the hemolytic activity, the PH series shows an initial decrease in activity, followed by a sharp increase as f_{alkyl} is increased, while the PB series shows a large initial decrease in activity with a subsequent steady increase. From the data it can be seen that the PH series is more active against human cell mimics than is the PB series. A direct comparison of the two series can be seen in Figure 33. As shown, as f_{alkyl} increases, the hemolytic activity of the PH series initially decreases, followed by a continual increase, which corresponds to the reported hemolytic activity of

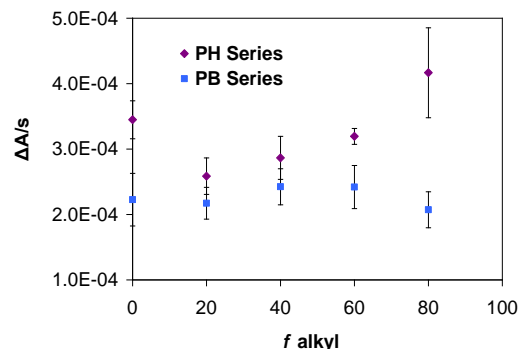


Figure 33: Comparison of kinetic response of hemolytic activity of the PH and PB series with varying f_{alkyl} values ($n=3$).

shows significantly less activity with the cholesterol-containing liposomes than those comprised of POPE/POPG. This suggests that the PB series, which contains shorter butyl-side chains than the hexyl-containing PH side chains, would have less toxicity towards human cells while demonstrating a higher selectivity for bacterial cells.

Initial and final images of the 29 min kinetic assay for antimicrobial activity of the synthetic polymers are shown in Figure 34.

These images not only show the distinctive color change in the presence of membrane permeabilizing polymeric agents as opposed to their absence, but also the degree of blue color that results from the relative ability of the polymers to permeate membranes. Therefore, not only can this new method be used as a visual detection

platform for screening antimicrobial activity of synthetic polymers, but it can also be used to visually detect the relative antimicrobial activity of these agents.

To determine the detection limits for this system, the most active polymers for each series against the egg PC, DOPA, and cholesterol liposomes were used, PH₅₁ and PB₅₄. Moreover, these polymers are good representations to use because their side chains are approximately 50%

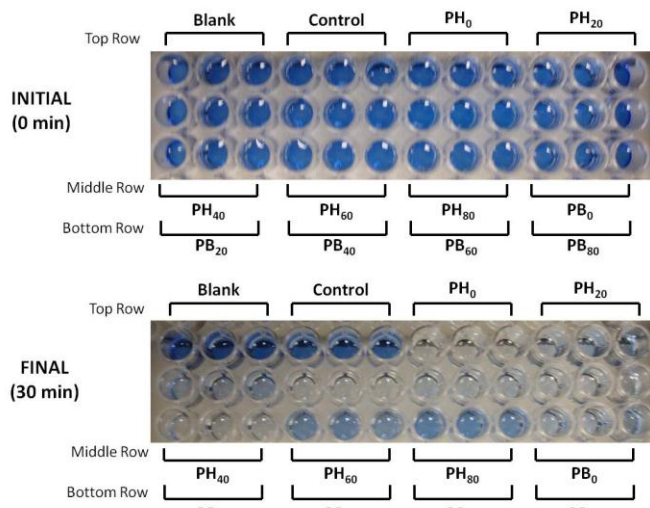


Figure 34: Visual detection of antimicrobial activity of the PH and PB series with varying falkyl values before and after 30min assay.

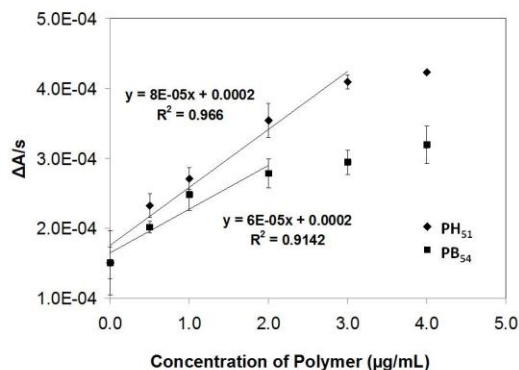


Figure 35: Linear dose response of PH₅₁ and PB₅₄ using egg PC, DOPA, and cholesterol liposomes. Detection limits for this system are 1.10 µg/mL (370 nM) for PH₅₁ and 1.47 µg/mL (490 nM) for PB₅₄.

alkylated, making them somewhat, but not completely, hydrophobic. For the dose-response assay, the concentration of the two polymers was varied from 0.5-4 $\mu\text{g/mL}$, and the response was monitored by a 29 min kinetic absorbance assay (Figure 35). This data also supports the generally higher activity of the PH series over the PB series. The limits of detection, based on three times the standard deviation of the control, were determined to be 1.10 $\mu\text{g/mL}$ (370 nM) for PH₅₁ and 1.47 $\mu\text{g/mL}$ (490 nM) for PB₅₄. Although the system appears to be able to detect polymers at a concentration below 1 $\mu\text{g/mL}$, the statistical detection limit is slightly above that value. However, the method is surely capable of detecting polymers at nano-molar levels.

Endpoint Assay for Polymer Activity

Along with kinetic response assays, the polymers were evaluated using the endpoint detection method, demonstrating the ability to adapt the system for a faster positive or negative

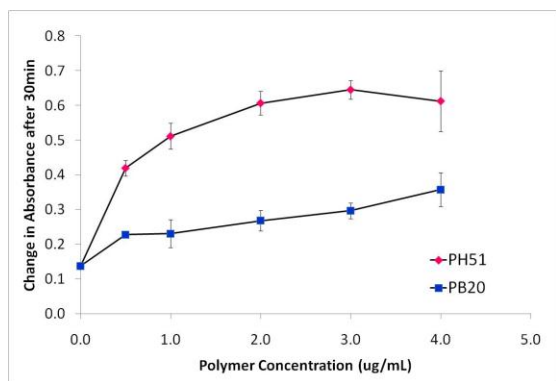


Figure 36: Endpoint assay for detection of antimicrobial activity of PH₅₁ and PB₂₀.

antimicrobial activity with POPE/POPG liposomes, PH₅₁ and PB₂₀ were used with concentrations varying from 0.5-4 $\mu\text{g/mL}$ (Figure 36). As expected, the rate of membrane permeation increases with concentration, with PH₅₁ being more active than PB₂₀. Images of the microtiter plate before and after the 30 min incubation are shown in Figure 37. It can be seen that wells containing polymer have undergone a significant color change as opposed to the dark

screening approach. As in the detection of MSI-594, an initial absorbance measurement was recorded, followed by a final absorbance measurement taken 30 min later. For each liposome composition, the most active polymer for

each series was used. For the detection of

blue control wells. Also, the wells containing PH₅₁ are considerably lighter in color than those containing PB₂₀, demonstrating that the relative activity of the polymers can be visually detected.

The polymers PH₅₁ and PB₅₄ were also used for the endpoint detection of hemolytic activity with egg PC, DOPA, and cholesterol

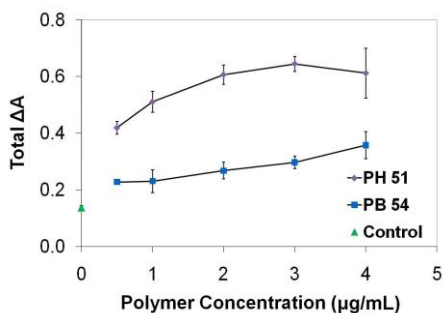


Figure 38: Endpoint assay for the detection of hemolytic activity of PH₅₁ and PB₅₄.

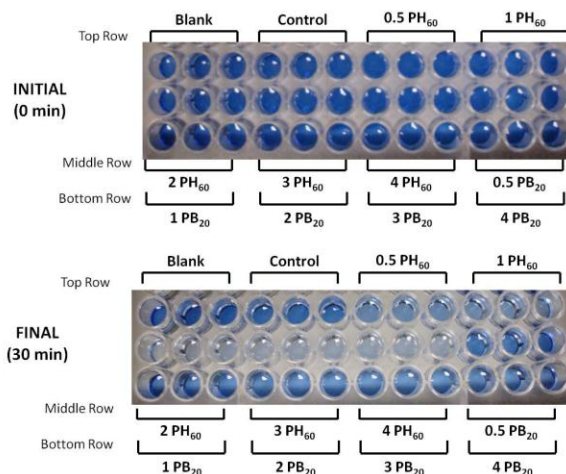


Figure 37: Visual detection of antimicrobial activity of PH₅₁ and PB₂₀ before and after 30 min endpoint assay.

liposomes, with concentrations ranging from 0.5-4 μg/mL (Figure 38). As before, the PH series is demonstrated to be more hemolytically active than the PB series.

Evaluation of Assay Using Gram-Positive Bacteria Liposome Mimics

The bacterial cell mimics used in the previous experiments were those of gram-negative bacteria, specifically the POPE/POPG liposomes mimicking *E. coli*. Along with bacteria that are considered to be gram-negative, there are gram-positive bacteria as well. Gram-positive bacteria contain a high amount of peptidoglycan in their cell walls, and are stained dark blue or violet by Gram staining (hence the term “gram-positive”)³⁶. Gram-negative bacteria, on the other hand, have an outer-membrane that contains large amounts of lipopolysaccharides. These bacteria do not retain the crystal violet dye in the Gram staining process (and are therefore “gram-negative”) and become translucent; they can, however, be counter-stained with a red dye. While there are more gram-negative bacteria species than there are gram-positive, many human-

pathogenic microbes are gram-positive, such as *Staphylococcus* and *Streptococcus*. The antimicrobial activity of the peptides and polymers against gram-positive bacteria was assessed using *S. aureus* cell mimics,

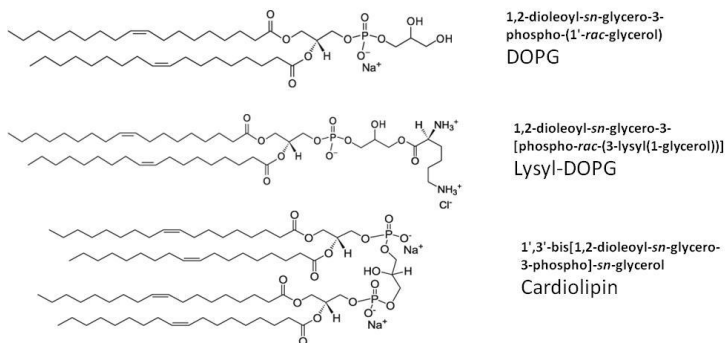


Figure 39: Lipid structures of DOPG, Lysyl-DOPG, and cardiolipin.

which were liposomes composed of a 12:7:1 mole ratio of DOPG:lysyl-DOPG:cardiolipin (CL) (Figure 39).

The antimicrobial activity against gram-positive bacteria was determined for the peptides MSI-594 and MSI-78 and the polymers PH₅₁ and PB₂₀. The polymers were chosen based on

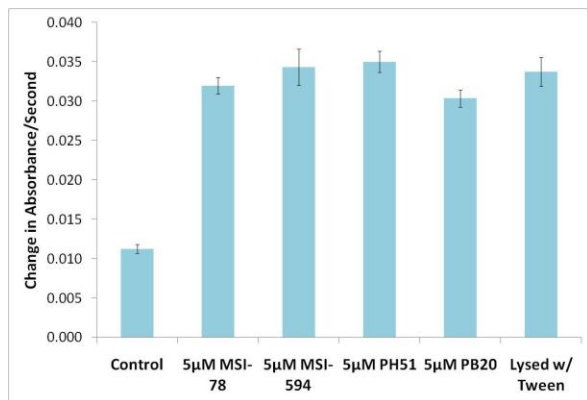


Figure 40: Membrane permeabilization of gram-positive cell mimics. The PQQ release caused by 5µM of each peptide and polymer was compared to that of liposomes lysed with Tween-20. Similar membrane lysis is demonstrated for the membrane-permeabilizing agents as is for the detergent.

their activity against gram-negative bacteria cell mimics (POPE/POPG liposomes). Liposomes were incubated with 5 µM of each peptide and polymer, and the response was monitored through a 29 min kinetic absorbance assay. The membrane permeation results were compared to liposomes lysed with Tween-20 (Figure 40). The assay shows a similar response to the peptides

and polymers as it does to the detergent Tween-20, but does not show a significant response from the control, demonstrating that this method can be applied to the detection of antimicrobial agents that target gram-positive bacteria.

Evaluation of DNP Model System for Complement Fixation Testing

Table 4: DNP Liposome Compositions

66:33:0.4 mole percent egg PC : cholesterol : DNP PE
33:33:33:1 mole percent egg PC : DOPA : cholesterol : DNP PE
44:44:11:1 mole percent egg PC : cholesterol : DOPA : DNP PE
44:44:11:1 mole percent egg PC : cholesterol : DOPA : DNP cap PE

Optimization of DNP Liposomes Lipid Composition

Four lipid compositions were tested for use in the DNP model system (Table 4). The liposomes were based on the previously characterized egg PC, DOPA, and cholesterol

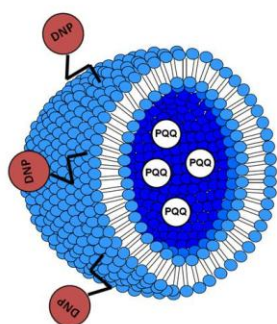


Figure 41: Structure of DNP-containing liposomes. The addition of a DNP-containing lipid should result in the presence of DNP molecules on the liposome surface.

liposomes, with the addition of a DNP-containing lipid (Figure 41). The first lipid composition did not contain the negatively charged DOPA lipid because it has been observed that negatively charged liposomes are susceptible to lysis by complement in absence of the appropriate antibody³⁷. However, while these liposomes showed an initial stability similar to that of egg PC, DOPA, and cholesterol liposomes, it was discovered that the liposomes



Liposomes aggregated in solution

aggregated in solution after sitting for a few days (Figure

Figure 42: Aggregation of egg PC, cholesterol and DNP PE liposomes in solution.

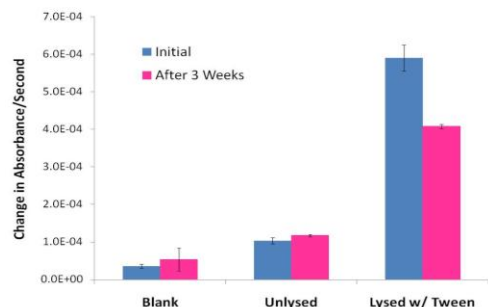


Figure 43: Stability of 33:33:33:1 mole percent egg PC:DOPA:cholesterol:DNP PE liposomes. After three weeks of refrigerated storage, there is not significant signal change in unlysed liposomes, suggesting the lipid membrane is still intact.

42). It is believed this aggregation was caused by the lack of any charged lipid, the presence of which results in repellent electrostatic forces between liposomes. In order to prevent aggregation, the lipid composition was altered to incorporate the negatively charged DOPA lipid. The liposomes composed of an equal mole ratio of

egg PC, DOPA, and cholesterol showed increased stability over those without DOPA, with a stable lifetime of three weeks at 4°C (Figure 43).

After establishing the stability of DNP-containing liposomes, a new liposome composition was tested taking into account the compromising effects of using a negatively charged lipid. The new liposomes were synthesized using a smaller amount of DOPA, resulting in a composition of 44:44:11:1 mole percent egg PC:cholesterol:DOPA:DNP PE. Even with the decreased amount of DOPA, these liposomes did not appear to aggregate and were determined to demonstrate a

similar stable lifetime to the previous lipid composition (Figure 44). While the two liposome compositions exhibit similar lifetimes to each other, it can be seen that the amount of PQQ released is significantly decreased after three weeks, which was not observed with previous liposome compositions that do not contain DNP. This decrease in PQQ

release suggests that, while the liposome membrane is not compromised after three weeks, the liposomes should be utilized during that time period to ensure adequate PQQ response in any lysing assay.

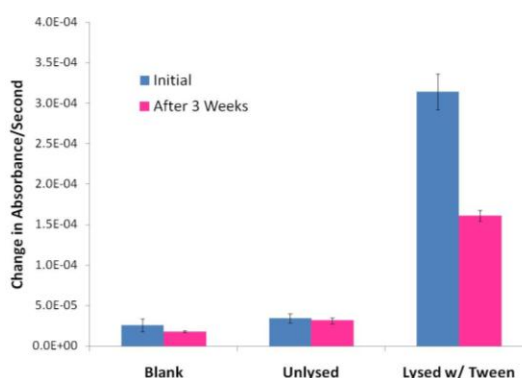


Figure 44: Stability of 44:44:11:1 egg PC:cholesterol:DOPA: DNP PE liposomes. After three weeks of refrigerated storage, there is not significant signal change in unlysed liposomes, suggesting the lipid membrane is still intact.

Finally, a fourth composition was tested which contained DNP Cap PE as the DNP-containing lipid as opposed to DNP PE. The DNP Cap PE lipid contains an extended linker

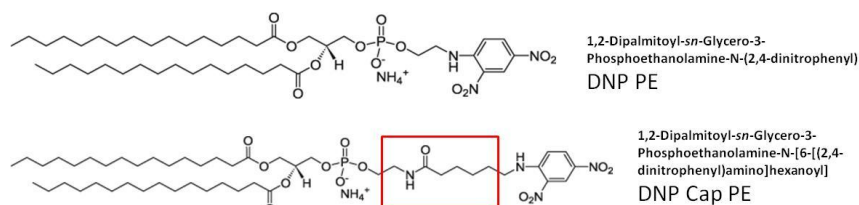


Figure 45: Lipid structures of DNP PE and DNP Cap PE. The extended linker chain present in DNP Cap PE is highlighted in red.

chain that holds the DNP molecule further from the lipid head (Figure 45). Liposomes containing

Cap-DNP were tested based on previous observations that Cap-DNP liposomes activate the alternate complement pathway (ACP) for guinea pig complement better than DNP liposomes³⁸. The Cap-DNP liposomes were determined to have a similar stable lifetime to the previous DNP liposomes, with little to no membrane degradation and PQQ leakage after three weeks.

The final two liposome compositions, containing either DNP PE or DNP Cap PE, were determined to encapsulate approximately 30 molecules of PQQ per liposome, which is about double the encapsulation efficiency of liposomes without DNP. However, these compositions contained a smaller mole ratio of the negatively charged DOPA lipid, which was suspected to reduce the encapsulation efficiency of liposomes due to repulsions between the negatively charged PQQ molecules and DOPA head groups. The increase of encapsulation efficiency corresponding to a decreased amount of DOPA lipid seems to support this initial theory.

UV-visible Absorbance of DNP liposomes

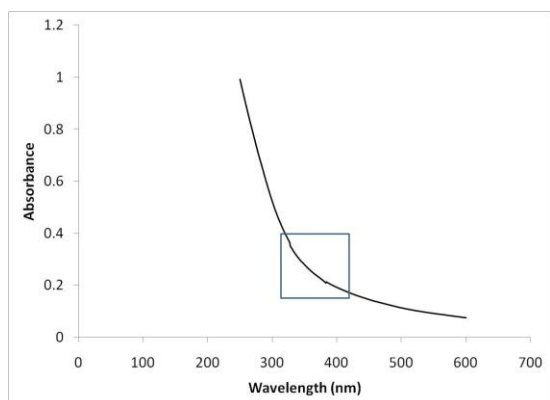


Figure 46: UV-visible spectrum of egg PC, DOPA, and cholesterol liposomes. The highlighted area shows no absorption between 335 nm and 385 nm.

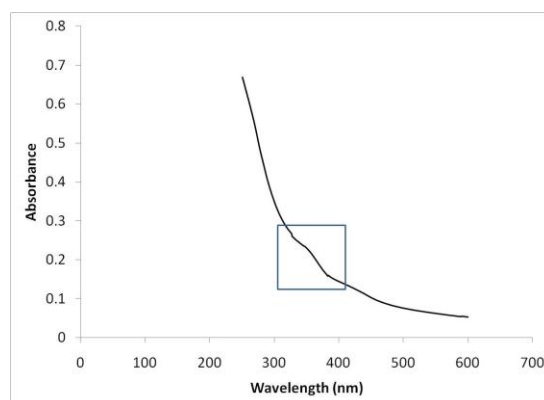


Figure 47: UV-visible spectrum of egg PC, DOPA, cholesterol, and DNP PE liposomes. The highlighted area shows an absorption change between 335 nm and 385 nm.

To determine if DNP molecules were present on the surface of liposomes, UV-visible absorbance spectra were taken of liposomes with and without a DNP-containing lipid (Figures 46 and 47). These spectra were compared to each other to determine if the addition of DNP PE

changed the liposome surface. A small absorbance change can be seen between 335 nm and 385 nm, which is highlighted on both spectra, suggesting the presence of something on the DNP liposome surface that is not present in liposomes that do not contain DNP. The reported absorbance maximum for DNP is located at 361 nm³⁹, which is within the range of the absorbance maximum seen in Figure 47. While this data suggests that DNP molecules are present on the surface of the liposomes containing DNP PE, it is not definitive and more tests are needed to confirm the presence of DNP on the liposome surface.

Competitive Binding Assay

In order to confirm the DNP molecules were present on the liposome surface and available for binding with anti-DNP antibodies, a competitive binding assay was employed (Figure 48). In

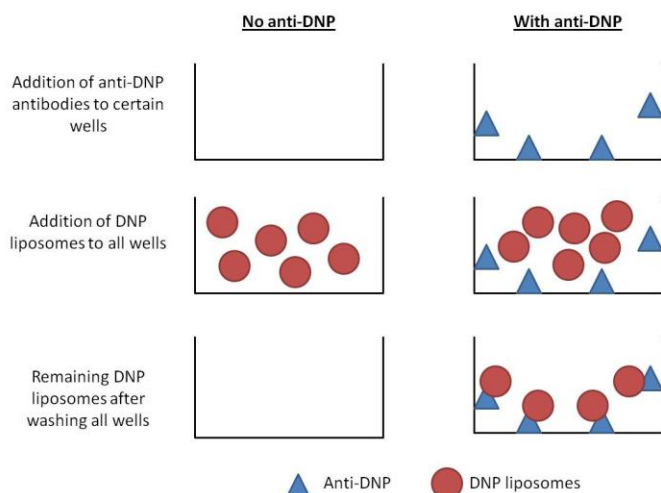


Figure 48: Competitive binding assay concept. In the presence of anti-DNP, DNP-containing liposomes should bind to the plate surface and lysis should result after the addition of Tween-20.

this assay, amine reactive microtiter plates were incubated with and without the presence of anti-DNP antibodies. If antibodies were present, they would react and attach to the microtiter plate. The excess anti-DNP was washed from the plate with buffer, and the remaining unreacted amine sites were capped with ethanolamine. At this point, liposomes

(either composed of a 33:33:33:1 mole percent of egg PC:DOPA:cholesterol:DNP PE or 1:1:1 mole ratio of egg PC:DOPA:cholesterol) were incubated in both the wells that contained and did not contain anti-DNP antibodies; after incubation, the wells were washed thoroughly to remove

any excess liposomes. If DNP was available for binding on the liposomes surface, the liposomes should remain bound to the anti-DNP on the surface of the microtiter plate after washing. If DNP was not available, no liposomes should remain in the well. Testing liposomes without DNP acted as a control to ensure that it is the DNP molecules on the liposome surface, and not the liposomes themselves, reacting with the antibody. The detergent Tween-20 was added to all wells to lyse any liposome present, resulting in a release of PQQ.

The results of the binding assay are shown in Figure 49. It can be seen that a signal is

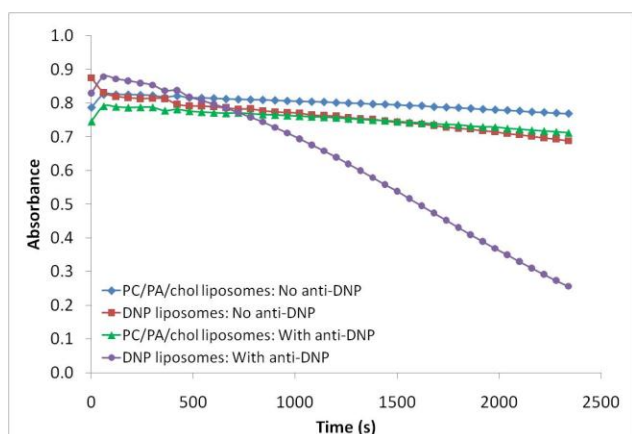


Figure 49: Competitive binding assay of egg PC, DOPA, and cholesterol liposomes with and without DNP PE. A signal is observed only when DNP-containing liposomes are in the presence of anti-DNP.

observed only in the case of the DNP liposomes in the presence of anti-DNP antibodies, with none of the controls resulting in surface bound liposomes reacting with the antibodies on the microtiter plate. Based on this, it can be concluded that the DNP molecules are not only present on the liposome surface, but are available and

capable of binding with the anti-DNP antibodies. Furthermore, these results demonstrate that the anti-DNP antibodies are interacting with the DNP molecules on the liposome surface, and not the lipid membrane, establishing the selectivity of the antibodies for the DNP molecules over other reagents in solution.

Complement Fixation Using DNP-Liposomes Loaded with PQQ

The long-term goal of this project was to develop a diagnostic assay for HIT that combines the selectivity of complement fixation with the sensitivity of the PQQ reconstitution assay. A

model system using liposomes composed of a DNP-containing lipid that should interact with anti-DNP antibodies was investigated first. Liposomes have previously been reported to interact with complement after antibody fixation at the surface⁴⁰, allowing the assay to retain the selectivity of the complement fixation test. The DNP molecules on the surface of PQQ-encapsulated liposomes should complex with both anti-DNP antibodies and complement in solution, resulting in membrane lysis and the release of PQQ.

Three liposome compositions (excluding the composition without DOPA) were tested, along with two types of complement for release of PQQ. The concentrations of antibody and complement in assay solution, as well as the time reagents were allowed to incubate, were varied. Liposomes composed of egg PC, DOPA, and cholesterol, without a DNP-containing lipid, were tested as well to determine if antibody and complement interacted with the lipid membrane in the absence of DNP.

Complement from human sera was initially used based on availability. However, the switch to guinea pig complement was made when no assay response was detected with the human sera complement. Furthermore, it has been previously reported that guinea pig ACP reacts more efficiently with DNP-Cap-liposomes than does human ACP³⁸.

The addition of anti-DNP antibodies and complement, both individually and simultaneously, to liposomes composed of a 1:1:1 mole ratio of egg PC:DOPA:cholesterol without a DNP-containing lipid did not result in liposome membrane lysis. The inability of the antibody and complement to complex and lyse liposomes without DNP demonstrates that the lipid membrane is not interacting with the complement in the absence of surface DNP molecules.

The optimization of the DNP model system was based on the variations in lipid composition, complement source, concentrations of antibody and complement, and length of

incubation time. However, a response to PQQ release based on the interaction between anti-DNP antibodies and complement with the DNP molecules on the liposome surface was not detected for this system. A representative result of the kinetic response for the DNP model

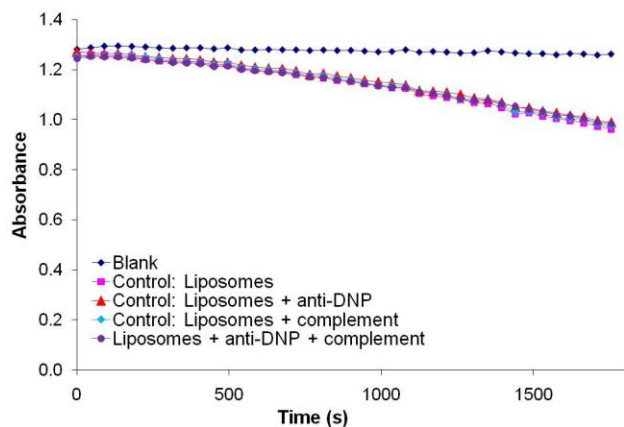


Figure 50: Representative spectrum of the kinetic response for the DNP model system. It can be seen that the response from the assay which should result in liposome lysis is not significantly different from the control responses.

system assay is shown in Figure 50. It can be seen that no significant difference is present between the controls (which should not result in membrane permeabilization) and the assay wells containing DNP liposomes, anti-DNP, and complement (which should complex and facilitate the release of PQQ). It was therefore concluded

that the optimization of the DNP model system based on these parameters did not result in any assay response, and proof-of-concept for this system was not attained.

Despite the unsuccessful attempt to optimize the DNP model system to detect complement fixation, there are remaining variables to be investigated. The liposome compositions containing egg PC, DOPA, and cholesterol were based on previous work with the PQQ assay system; however, they do not coincide with the lipid compositions reported in the literature that is used for complement tests^{38,40-41}. Using a previously proven lipid composition for DNP/anti-DNP complement fixation may result in better interactions between DNP molecules, antibodies, and complement, leading to the expected assay response. Similarly, removing the negatively charged lipid DOPA, which is known to facilitate liposome activation by complement without antibody present, from the composition and instead incorporating a positively charged lipid (to maintain aggregation prevention) may yield better results. Furthermore, dramatically increasing the

amount of DNP lipid within the liposome may lead to more interactions between DNP molecules and anti-DNP antibodies. However, with this increase it may be necessary to optimize the amount of DNP lipid to avoid steric effects. It is also possible that the small size of the liposomes (approximately 150 nm in diameter) may be causing steric effects that are preventing the DNP, anti-DNP, and complement complex from forming the required ternary complex. Increasing the liposome size may help to reduce any steric hindrances that may be present and result in greater antibody and complement interaction with the DNP molecules on the liposome surface. Although the DNP model system has not yet resulted in the assay response expected, there are still many variables that can be investigated to further attempt the optimization of this system.

CONCLUSIONS

The GDH reconstitution assay using PQQ-encapsulated liposomes as cell mimics is a simple and sensitive platform for the detection of membrane permeabilization by antimicrobial agents such as peptides and synthetic copolymers. The method demonstrated high selectivity for the active peptides MSI-594 and MSI-78 over the inactive control peptide rIAPP, allowing it to be a simple method to determine the relative antimicrobial activity of different peptides. Using a 30 min endpoint detection assay, active peptide MSI-594 can be detected at concentrations as low as 396 nM, which is comparable to the sensitivity of current detection methods that use fluorescent dye-loaded liposomes. Furthermore, the optical nature of the assay allows for a visual detection of membrane lysis, allowing the simple screening of peptide activity without the use of expensive and complicated instrumentation.

The antimicrobial activity of the PH and PB polymer series, each with varying degrees of side chain alkylation, was investigated as well. The effect of hydrophobicity on the antimicrobial activity of the polymer was easily determined by this method, with PH₅₁ and PB₂₀ demonstrating the highest activity for each series. Similarly, the effect of hydrophobicity on the hemolytic activity of both polymer series was determined as well, with PH₅₁ and PB₅₄ exhibiting the most potential toxicity towards mammalian cells. Similar to the peptide detection, the assay method is capable of detecting copolymers at nano-molar levels, with limits of detection of 370 nM for PH₅₁ and 490 nM for PB₅₄.

Along with the ability to detect membrane permeabilization in both mammalian and gram negative bacteria cell mimics, the new assay method was employed to detect the permeation of gram positive bacteria cell mimic membranes as well. This method can therefore be used to detect antimicrobial agents that target both gram positive and gram negative bacteria, as well as

determine the potential toxicity of those agents against mammalian cells. This method should be an attractive tool for the determination of antimicrobial activity of both new antimicrobial entities and already known species such as amyloid peptides or toxins.

While proof-of-concept and optimization of the DNP model system for complement fixation (aimed at developing a new type of HIT detection method) was not achieved, progress was made in the direction of system optimization. It was determined that DNP molecules are present on the surface of the liposomes and are capable of binding with anti-DNP antibodies. It was also determined that the antibodies are interacting with the DNP molecules themselves, and not the lipid membrane of the liposomes, establishing the selectivity of the antibodies for DNP molecules. Although the effort to optimize the DNP model system was not successful, there are still several research directions to pursue to demonstrate the concept of the proposed system.

REFERENCES

- ¹Fleming, A. "On the antibacterial action of cultures of a penicillium, with special reference to their use in the isolation of *B. influenzae*" *Bull. World Health Organ.*, **2001**, 79, 780-790.
- ²McPhee, J.B.; Hancock, R.E.W. "Function and therapeutic potential of host defense peptides" *J. Pept. Sci.*, **2004**, 11, 677-687.
- ³Hancock, R.E.W.; Diamond, G. "The role of cationic antimicrobial peptides in innate host defenses" *Trends Microbiol.*, **2000**, 8, 402-410.
- ⁴Zasloff, M. "Antimicrobial peptides of multicellular organisms" *Nature*, **2002**, 415, 389-395.
- ⁵Marr, A.K.; Gooderham, W.J.; Hancock, R.E.W. "Antibacterial peptides for therapeutic use: obstacles and realistic outlook" *Curr. Opin. PHarmacol.*, **2006**, 6, 468-472.
- ⁶Palermo, E.F.; Kuroda, K. "Chemical structure of cationic groups in amphiphilic polymethacrylates modulates the antimicrobial and hemolytic activities" *Biomacromolecules*, **2009**, 10, 1416-1428.
- ⁷Palermo, E.F.; Sovadinova, I.; Kuroda, K. "Structural determinants of antimicrobial activity and biocompatibility in membrane-disrupting methacrylamide random copolymers" *Biomacromolecules*, **2009**, 10, 3098-3107.
- ⁸Almeida, P.F.; Pokorny, A. "Mechanisms of antimicrobial cytolytic and cell-penetrating peptides: from kinetics to thermodynamics" *Biochemistry*, **2009**, 48, 8083-8093.
- ⁹Chen, R.F.; Knutson, J.R. "Mechanism of fluorescence concentration quenching of carboxyfluorescein in liposomes: energy transfer to nonfluorescent dimmers" *Anal. Biochem.*, **1988**, 172, 61-77.
- ¹⁰Rausch, J.M.; Wimley, W.C. "A high-throughput screen for identifying transmembrane pore-forming peptides" *Anal. Biochem.*, **2001**, 293, 258-263.
- ¹¹Kroupis, C.; Theodorou, M.; Kounavi, M.; Oliveira, S.C.; Iliopoulou, E.; Mavri-Vavayanni, M.; Melissari, E.N.; Degiannis, D. "Development of a real-time PCR detection method for a FCGR2A polymorphism in the LightCycler and application in the heparin-induced thrombocytopenia syndrome" *Clinical Biochem.*, **2009**, 42, 1685-1693.
- ¹²Polgár, J.; Eichler, P.; Greinacher, A.; Clemetson, K.J. "Adenosine diphosphate (ADP) and ADP receptor play a major role in platelet activation/aggregation induced by sera from heparin-induced thrombocytopenia patients" *Blood*, **1998**, 91, 549-554.
- ¹³Vitale, M.; Tazzari, P.; Ricci, F.; Mazza, M.A. ; Zauli, G. ; Martini, G. ; Caimi, L. ; Manzoli, F.A. ; Conte, R. "Comparison between different laboratory tests for the detection and prevention of heparin-induced thrombocytopenia" *Cytometry*, **2001**, 46, 290-295.
- ¹⁴Isben, L.M. "Organ System Issues and Specific Diseases Commonly Encountered in the PICU" www.ohsu.edu/academic/picu/common%20conditions.htm 2002.
- ¹⁵Sheridan, D.; Carter, C.; Kelton, J.G. "A diagnostic test for heparin-induced thrombocytopenia" *Blood*, **1986**, 67, 27-30.
- ¹⁶Rao, C.V. *Immunology*. Alpha Science Internation, Ltd.: Middlesex. 2005, 112-113.

- ¹⁷Bangham, A.D.; Standish, M.M.; Watkins, J.C. "Diffusion of univalent ions across the lamellae of swollen phospholipids" *J. Mol. Biol.*, **1965**, *13*, 238-252, IN26-IN27.
- ¹⁸Jesorka, A.; Orwar, O. "Liposomes: Technologies and Analytical Applications" *Annu. Rev. Anal. Chem.*, **2008**, *1*, 801-832.
- ¹⁹Gomez-Hens, A.; Fernandez-Romero, J.M. "The role of liposomes in analytical processes" *TrAC Trends in Analytical Chemistry*, **2005**, *24*, 9-19.
- ²⁰Singh, A.K.; Kilpatrick, P.K.; Carbonell, R.G. "Applications of antibody and fluorophore-derivatized liposomes to heterogeneous immunoassays for D-dimer" *Biotechnol. Prog.*, **1996**, *12*, 272-280.
- ²¹Morris, D.L.; Ellis, P.B.; Carrico, R.J.; Yeager, F.M.; Schroeder, H.R.; Albarella, J.P.; Boguslaski, R.C.; Hornby, W.E.; Rawson, D. "Flavin adenine dinucleotide as a label in homogeneous colorimetric immunoassays" *Anal. Chem.*, **1981**, *53*, 658-665.
- ²²Salisbury, S.A.; Forrest, H.S.; Cruse, W.B.T.; Kennard, O. "A novel coenzyme from bacterial primary alcohol dehydrogenases" *Nature*, **1979**, *280*, 843-844.
- ²³Davidson, V. (ed.) *Principles and Applications of Quinoproteins*. Marcel Dekker, Inc.: New York. 1993, 47-50.
- ²⁴Oubrie, A.; Rozeboom, H.T.J.; Kalk, K.H.; Olsthoorn, A.J.J.; Duine, J.A.; Dijkstra, B.W. "Structure and mechanism of soluble quinoprotein glucose dehydrogenase" *EMBO J.*, **1999**, *18*, 5187-5194.
- ²⁵Shen, D.; Meyerhoff, M.E. "Pyrroloquinoline quinone-doped polymeric nanospheres as sensitive tracer for binding assays" *Anal. Chem.*, **2009**, *81*, 1564-1569.
- ²⁶Porcelli, F.; Buck-Koehntop, B.A.; Thennarasu, S.; Ramamoorthy, A.; Veglia, G. "Structures of the dimeric and monomeric variants of magainin antimicrobial peptides (MSI-78 and MSI-594) in micelles and bilayers, determined by NMR spectroscopy" *Biochemistry*, **2006**, *45*, 5793-5799.
- ²⁷Ramamoorthy, A.; Thennarasu, S.; Lee, D.K.; Tan, A.; Maloy, L. "Solid-state NMR investigation of the membrane-disrupting mechanism of antimicrobial peptides MSI-78 and MSI-594 derived from magainin 2 and melittin" *Biophysics J.*, **2006**, *91*, 206-216.
- ²⁸Brender, J.R.; Hartman, K.; Reid, K.R.; Kennedy, R.T.; Ramamoorthy, A. "A single mutation in the nonamyloidogenic region of islet amyloid polypeptide greatly reduces toxicity" *Biochemistry*, **2008**, *47*, 12680-12688.
- ²⁹Nanga, R.P.; Brender, J.R.; Xu, J.; Hartman, K.; Subramanian, V.; Ramamoorthy, A. "Three-dimensional structure and orientation of rat islet amyloid polypeptide protein in a membrane environment by solution NMR spectroscopy" *J. Am. Chem. Soc.*, **2009**, *131*, 8252-8261.
- ³⁰Szoka, F.; Papahadjopoulos, D. "Comparative properties and methods of preparation of lipid vesicles (liposomes)" *Annu. Rev. Biophys.*, **1980**, *9*, 467-508.
- ³¹Bartlett, G.R. "Phosphorus assay in column chromatography" *J. Biol. Chem.*, **1959**, *234*, 466-468.

- ³²Zimmerman, L.B.; Lee, K-D.; Meyerhoff, M.E. “Visual detection of single-stranded target DNA using pyrroloquinoline quinone-loaded liposomes as a tracer” *Anal. Biochem.*, **2010**, *401*, 182-187.
- ³³Papahadjopoulos, D.; Nir, S.; Duzgunes, N. “Molecular mechanisms of calcium-induced membrane fusion” *J. Bioenerg.*, **1990**, *22*, 157-179.
- ³⁴Wilschut, J.; Papahadjopoulos, D. “Ca²⁺-induced fusion of phospholipid vesicles monitored by mixing of aqueous contents” *Nature*, **1979**, *281*, 690-692.
- ³⁵Yazdanbakhsh, K.; Lomas-Francis, C.; Reid, M.E. “Blood groups and diseases associated with inherited abnormalities of the red blood cell membrane” *Transfusion Med. Rev.*, **2000**, *14*, 364-374.
- ³⁶Schaechter, M.; Ingraham, J.L.; Neidhardt, F.C. *Microbe*. ASM Press: Washington, D.C. 2006, 23-28.
- ³⁷Rongen, H.A.H.; Bult, A.; van Bennekom, W.P. “Liposomes and immunoassays” *J. Immun. Methods.*, **1997**, *204*, 105-133.
- ³⁸Okada, N.; Yasuda, T.; Tsumita, T.; Okada, H. “Differing reactivities of human and guinea-pig complement on haptized liposomes via the alternative pathway” *Molecular Immunology*, **1983**, *20*, 857-864.
- ³⁹Park, S.N.; Kim, C.S.; Kim, M.H.; Lee, I.J.; Kim, K. “Spectrophotometric measurement of the first dissociation constants of carbonic acid at elevated temperature” *J. Chem. Soc., Faraday Trans.*, **1998**, *94*, 1421-1425.
- ⁴⁰Aragno, D.; Leserman, L.D. “Immune clearance of liposomes inhibited by an anti-Fc receptor antibody *in vivo*” *Proc. Natl. Acad. Sci.*, **1986**, *83*, 2699-2703.
- ⁴¹Yamamoto, S.; Kubotsu, K.; Kida, M.; Kondo, K.; Matsuura, S.; Uchiyama, S.; Yonekawa, O.; Kanno, T. “Automated homogeneous liposome-based assay system for total complement activity” *Clin. Chem.*, **1995**, *41*, 586-590.